

# Four-particle solutions to Baxter equation of $SL(2, \mathbb{C})$ Heisenberg spin magnet for integer conformal Lorentz spin and their normalizability

JAN KOTANSKI<sup>†</sup>

The four reggeized gluon states for non-vanishing Lorentz conformal spin  $n_h$  are considered. To calculate their spectrum the  $Q$ -Baxter method is used. As a result we describe normalizable trajectory-like states, which form continuous spectrum, as well as discrete point-like solutions, which turn out to be non-normalizable. The point-like solutions exist due to symmetry of the Casimir operator where conformal weights  $(h, \bar{h}) \rightarrow (h, 1 - \bar{h})$ .

PACS numbers: 12.40.Nn, 11.55.Jy, 12.38.-t, 12.38.-t

*Keywords:* Reggeons, QCD, spectrum, eigenstates

TPJU-2/2007

## 1. Introduction

In high energy limit of QCD the scattering processes can be described by means of effective particles that are compound states of reggeized gluons, shortly Reggeons [1, 2, 3]. In calculations of the scattering processes of hadrons with  $N$ -Reggeon exchange one can find that the high energy asymptotics of the scattering amplitude is governed by intercepts [2, 3]. On the other hand, applying reggeized gluons to deep inelastic processes one can compute anomalous dimensions of QCD for the hadron structure function [4, 5, 6].

To find the intercepts as well as the anomalous dimensions the BKP equation is considered [7], which is a generalization of the BFKL equation [3] to multi-Reggeon exchange. This equation has a structure of a Schrödinger equation and it corresponds to the non-compact Heisenberg  $SL(2, \mathbb{C})$ -spin

---

<sup>†</sup> Institute of Physics, Jagellonian University, Reymonta 4, PL-30-059 Cracow, Poland

magnet. The energy in this equation is called the Reggeon energy while the eigenfunctions are the Reggeon wave-functions. To solve the BKP equation one can equivalently calculate solutions of the Baxter  $Q$ -operator eigenproblem [8, 9] defined by Baxter equations [10, 11, 12]. The system is completely integrable, it possesses a complete set of integrals of motion, *i.e.* conformal charges  $\{q_k, \bar{q}_k\}$  with  $k = 2, \dots, N$ . Therefore, the energy is a function of these conformal charges. Eigenvalues of the lowest conformal charges, *i.e.*  $(q_2, \bar{q}_2)$ , depend on conformal weights  $(h, \bar{h})$  which are parameterized by the real scaling dimension  $\nu_h$  and the integer conformal Lorentz spin  $n_h$ . Additionally, applying the WKB approach [12], which consists in constructing the asymptotic solutions to Baxter equations, one finds that the remaining conformal charges are parameterized by additional set of  $(2N - 4)$ -integer parameters. For fixed  $(h, \bar{h})$  these integer numbers enumerate vertices of WKB lattices which correspond to higher conformal charges [12, 13]. Since the solutions depend on continuous parameter  $\nu_h$  the remaining conformal charges  $q_3, \dots, q_N$  form one-dimensional trajectories in the conformal charge space.

In this work we focus on four-Reggeon exchanges which have been described in the following references [11, 13, 14, 6]. The intercept of these exchanges is defined by the minimal energy as  $\alpha(0) = 1 - \min(E_4)\alpha_s N_c/(4\pi)$ . Contrary to Ref. [11] the authors of Ref. [15] claim that the leading contribution in the  $N = 4$  Reggeon sector comes from the exchange with  $n_h = 2$  with the intercept higher than the intercept of the BFKL-pomeron. Here we intend to explain these results. Thus, we analyse the energy spectrum of the exchanged states and calculate the spectrum of the conformal charges with  $n_h \in \mathbb{Z}$ . Indeed, it turns out that additionally to the ordinary trajectory states, there exist other solutions to the Baxter equations. These solutions appear only for  $n_h \neq 0$  and are not situated on any trajectory, *i.e.* they are point-like. Moreover, their conformal charges correspond to the results of Refs. [6, 15].

In order to contribute to the scattering amplitude processes, *i.e.* to be physical, the solutions should be normalizable according to the  $SL(2, \mathbb{C})$  scalar product. Thus, the scalar product of the trajectory solutions with continuous parameters  $\nu_h$  and  $\nu'_h$  has to be proportional to  $\delta(\nu_h - \nu'_h)\delta_{n_h n'_h}$ , while the scalar products of the point-like solutions to the Kronecker delta  $\delta_{n_h n'_h}$ . On the other hand, by construction, the wave functions of the eigenstates should have transformation property with respect to  $SL(2, \mathbb{C})$  conformal transformations, *i.e.* they have to be homogeneous functions of two-dimensional coordinates and must not involve any scale. Therefore, the product of two eigenstates could be either 0 or  $\infty$ . If the eigenstates are continuous in  $\nu_h$  (trajectory-like solutions), then 0 or  $\infty$  follows from the Dirac delta function. If the eigenstates are discrete either the norm of each

eigenstate is infinite and this means that this state does not contribute to the decomposition of the Hamiltonian over the eigenstates, or the eigenstates and/or the scalar product involve some scale, which breaks conformal symmetry. However, as will be shown in the following, the point-like solutions have infinite norm so these solutions are not normalizable w.r.t.  $\text{SL}(2, \mathbb{C})$  scalar product.

The existence of non-normalizable states may be understood by performing analytical continuation of the physical trajectory solutions from the  $n_h = 0$  sector to the complex  $\nu_h$ -plane which implies relaxation of the normalization condition. It turns out that due to a symmetry of the Casimir operator, solutions from this analytical continuation plane with  $i\nu_h \in \mathbb{Z}/2$  have their twin-solutions with  $\nu_h = 0$  and  $n_h \in \mathbb{Z}$ . These twin-solutions have the same conformal charges as the corresponding solutions from the  $n_h = 0$  analytical plane. They differ only in the conformal weight with  $\bar{h} \rightarrow 1 - \bar{h}$ . The latter transformation may move states outside the normalizable physical range. Therefore, some twin-solutions, *i.e.* point-like ones, as will be shown in the following, are non-normalizable.

The energy of the ground state gives the largest contribution to the scattering amplitude. Assuming that this ground state is not degenerated implies  $q_3 = 0$  [16]. Usually the trajectory solutions have the lowest energy at  $\nu_h = 0$ . Moreover, the energy of the trajectory solution with  $n_h \neq 0$  is always higher than the minimal energy of the states from the  $n_h = 0$  sector. For even  $n_h$  and  $q_3 = 0$  the normalizable solutions coexist with non-normalizable ones. Here, the point-like solutions do not correspond to WKB lattices and their number for fixed  $n_h$  equals  $|n_h/2|$ . The point-like solution with the lowest energy belongs to the  $n_h = 4$  sector and its energy is comparable to two-Pomeron exchange energy. On the other hand we have found that all solutions with odd  $n_h$  and  $q_3 = 0$  are point-like and non-normalizable, and can be described by vertices of WKB lattices.

In this work we compute numerically the Hamiltonian spectra of four reggeized gluons. As a result we get trajectory solutions to the Baxter equations which form continuous spectra. Moreover, we also find the point-like solutions. We try to look more closely at their origin and discuss their normalizability conditions. In Section 2 the Reggeon Hamiltonian is introduced and the way of finding its spectrum using the Baxter method is shown. In the next section the integral ansatz is applied to rewrite the Baxter equations in a differential form and find their solutions. Moreover, the  $\text{SL}(2, \mathbb{C})$ -norm is evaluated. In Section 4 the normalizable trajectory-like solution are presented and analytical continuation to the complex  $\nu_h$ -plane is performed. Furthermore, the symmetry between solutions with (half-)integer conformal charges is established. In Section 5 trajectory-like solutions at the specific point  $\nu_h = 0$  are discussed. Furthermore, in Section 6 non-normalizable

point-like solutions are constructed. They also appear at  $\nu_h = 0$ . However, they are not situated on any trajectory and we check they are non-normalizable. At the end we add final conclusions.

## 2. Hamiltonian and the Baxter operator

### 2.1. Hamiltonian

In the high energy Regge limit the total energy  $s \rightarrow \infty$  and the four-momentum transfer  $t$  is constant. In this limit the contribution of  $N = 4$  reggeized gluons to the scattering amplitude can be written as:

$$\mathcal{A}_{N=4}(s, t) = s \int d^2 z_0 e^{i \vec{z}_0 \cdot \vec{p}} \langle \Phi_A(\vec{z}_0) | e^{-\bar{\alpha}_s Y \mathcal{H}_4/4} | \Phi_B(0) \rangle, \quad (1)$$

where the rapidity  $Y = \ln s$  and  $\bar{\alpha}_s = \alpha_s N_c / \pi$  is the strong coupling constant. The wave-functions  $|\Phi_{A(B)}(\vec{z}_0)\rangle \equiv \Phi_{A(B)}(\vec{z}_i - \vec{z}_0)$  describe the coupling of four gluons to the scattered particles. The  $\vec{z}_0$ -integration fixes the momentum transfer  $t = -\vec{p}^2$ . In the multi-colour limit [17] the Hamiltonian

$$\mathcal{H}_4 = H_4 + \bar{H}_4, \quad [H_4, \bar{H}_4] = 0. \quad (2)$$

Holomorphic and anti-holomorphic Hamiltonians can be written in the Möbius representation [18, 9] as

$$H_4 = \sum_{k=1}^4 H(J_{k,k+1}), \quad \bar{H}_4 = \sum_{k=1}^4 H(\bar{J}_{k,k+1}), \quad (3)$$

where

$$H(J) = \psi(1 - J) + \psi(J) - 2\psi(1), \quad (4)$$

with  $\psi(x) = d \ln \Gamma(x) / dx$  being the Euler digamma function and  $J_{4,5} = J_{4,1}$ . The operators,  $J_{k,k+1}$  and  $\bar{J}_{k,k+1}$ , are defined through the Casimir operators for the sum of the  $\text{SL}(2, \mathbb{C})$  spins related to the neighbouring Reggeons [10]

$$J_{k,k+1}(J_{k,k+1} - 1) = (S^{(k)} + S^{(k+1)})^2, \quad (5)$$

with  $S_\alpha^{(5)} = S_\alpha^{(1)}$ , and  $\bar{J}_{k,k+1}$  is defined similarly.

The high energy behaviour of the scattering amplitude (1) is governed by the eigenvalues of  $\mathcal{H}_4$ , which are also called Reggeon energies,  $E_4(q, \bar{q})$ . In order to find  $E_4(q, \bar{q})$  one has to solve the Schrödinger equation

$$\mathcal{H}_4 \Psi_{\vec{p}, \{q, \bar{q}\}}(\vec{z}_1, \vec{z}_2, \vec{z}_3, \vec{z}_4) = E_4(q, \bar{q}) \Psi_{\vec{p}, \{q, \bar{q}\}}(\vec{z}_1, \vec{z}_2, \vec{z}_3, \vec{z}_4), \quad (6)$$

where different energy values are enumerated by quantum numbers  $\{q, \bar{q}\} \equiv (q_2, q_3, q_4, \bar{q}_2, \bar{q}_3, \bar{q}_4)$ . The eigenstates  $\Psi_{\vec{p}, \{q, \bar{q}\}}(\vec{z}_1, \vec{z}_2, \vec{z}_3, \vec{z}_4)$  are single-valued functions on the planes  $\vec{z}_i = (z_i, \bar{z}_i)$ , normalizable with respect to the  $\text{SL}(2, \mathbb{C})$  invariant scalar product

$$\langle \Psi_{\vec{p}, \{q, \bar{q}\}} | \Psi_{\vec{p}, \{q, \bar{q}\}} \rangle = \int d^2 z_1 d^2 z_2 d^2 z_3 d^2 z_4 |\Psi_{\vec{p}, \{q, \bar{q}\}}(\vec{z}_1, \vec{z}_2, \vec{z}_3, \vec{z}_4)|^2, \quad (7)$$

where  $d^2 z_i = dx_i dy_i = dz_i d\bar{z}_i / 2$  with  $\bar{z}_i = z_i^*$ <sup>1</sup>.

## 2.2. Baxter operator

In order to solve the Schrödinger equation (6) one can apply the powerful method of the Baxter  $Q$ -operator [19, 10]. This operator depends on two complex spectral parameters  $u, \bar{u}$  and in the following will be denoted as  $\mathbb{Q}(u, \bar{u})$ . By definition  $\mathbb{Q}(u, \bar{u})$  has to satisfy the commutativity relations

$$[\mathbb{Q}(u, \bar{u}), \mathbb{Q}(v, \bar{v})] = 0, \quad (8)$$

and

$$[\hat{t}_4(u), \mathbb{Q}(u, \bar{u})] = [\hat{t}_4(\bar{u}), \mathbb{Q}(u, \bar{u})] = 0, \quad (9)$$

as well as Baxter equations

$$\hat{t}_4(u) \mathbb{Q}(u, \bar{u}) = (u + is)^4 \mathbb{Q}(u + i, \bar{u}) + (u - is)^4 \mathbb{Q}(u - i, \bar{u}), \quad (10)$$

$$\hat{t}_4(\bar{u}) \mathbb{Q}(u, \bar{u}) = (\bar{u} + i\bar{s})^4 \mathbb{Q}(u, \bar{u} + i) + (\bar{u} - i\bar{s})^4 \mathbb{Q}(u, \bar{u} - i), \quad (11)$$

where the auxiliary transfer matrices

$$\hat{t}_4(u) = 2u^4 + \hat{q}_2 u^2 + \hat{q}_3 u + \hat{q}_4, \quad (12)$$

and similarly for  $\hat{t}_4(\bar{u})$ , are polynomials in spectral parameter  $u$  with the coefficients being the integrals of motion, *i.e.* conformal charges. In the QCD case the complex spins  $(s, \bar{s}) = (0, 1)$ .

The operators of conformal charges have a particularly simple form for the  $\text{SL}(2, \mathbb{C})$  spins  $s = 0$ :

$$\hat{q}_k = i^k \sum_{1 \leq j_1 < j_2 < \dots < j_k \leq 4} z_{j_1 j_2} \dots z_{j_{k-1} j_k} z_{j_k j_1} \partial_{z_{j_1}} \dots \partial_{z_{j_{k-1}}} \partial_{z_{j_k}}, \quad (13)$$

as well as for  $\bar{s} = 1$ :

$$\hat{\bar{q}}_k = i^k \sum_{1 \leq j_1 < j_2 < \dots < j_k \leq 4} \partial_{\bar{z}_{j_1}} \dots \partial_{\bar{z}_{j_{k-1}}} \partial_{\bar{z}_{j_k}} \bar{z}_{j_1 j_2} \dots \bar{z}_{j_{k-1} j_k} \bar{z}_{j_k j_1}. \quad (14)$$

---

<sup>1</sup> Here *bar* is used to denote quantities in the anti-holomorphic sector, whereas the *asterisk* denotes complex conjugation

with  $z_{ij} = z_i - z_j$  and  $\bar{z}_{ij} = \bar{z}_i - \bar{z}_j$ . Eigenvalues of the lowest conformal charges,

$$q_2 = -h(h-1), \quad \text{and} \quad \bar{q}_2 = -\bar{h}(\bar{h}-1), \quad (15)$$

are parameterized by conformal weight

$$h = \frac{1+n_h}{2} + i\nu_h, \quad \bar{h} = \frac{1-n_h}{2} + i\nu_h, \quad (16)$$

where integer  $n_h$  has a meaning of the two-dimensional Lorentz spin, whereas  $\nu_h$  defines the scaling dimension. Note that the complex spins  $(s, \bar{s})$  and conformal weights  $(h, \bar{h})$  parameterize the irreducible representations of the  $\text{SL}(2, \mathbb{C})$  group.

The Baxter  $\mathbb{Q}(u, \bar{u})$ -operator as well as the Hamiltonian (2) commute with the auxiliary transfer matrices (9), and as a consequence they share the common set of eigenfunctions. Moreover, the eigenvalues of the  $Q$ -operator, defined by

$$\mathbb{Q}(u, \bar{u}) \Psi_{\vec{p}, \{q, \bar{q}\}}(\vec{z}_1, \vec{z}_2, \vec{z}_3, \vec{z}_4) = Q_{q, \bar{q}}(u, \bar{u}) \Psi_{\vec{p}, \{q, \bar{q}\}}(\vec{z}_1, \vec{z}_2, \vec{z}_3, \vec{z}_4), \quad (17)$$

satisfy the same Baxter equations (10) and (11) with the auxiliary transfer matrices replaced by their corresponding eigenvalues. Thus, to find the eigenvalues of the  $Q$ -operator we solve the eigenproblem of the Hamiltonian (2), which can be written in terms of the Baxter  $Q$ -operator [10]:

$$\mathcal{H}_4 = \epsilon_4 + i \frac{d}{du} \ln \mathbb{Q}(u + is, \bar{u} + i\bar{s}) \Big|_{u=0} - \left( i \frac{d}{d\bar{u}} \ln \mathbb{Q}(u - is, \bar{u} - i\bar{s}) \Big|_{u=0} \right)^\dagger, \quad (18)$$

where the additive normalization constant is given as

$$\epsilon_4 = 8 \operatorname{Re}[\psi(2s) + \psi(2 - 2s) - 2\psi(1)]. \quad (19)$$

Finally, the Hamiltonian (2) is invariant under cyclic and mirror permutations [10] defined by

$$\begin{aligned} \mathbb{P} \Psi_{\{q, \bar{q}\}}(\vec{z}_1, \vec{z}_2, \dots, \vec{z}_4) &\stackrel{\text{def}}{=} \Psi_{\{q, \bar{q}\}}(\vec{z}_2, \vec{z}_3, \dots, \vec{z}_1) \\ &= e^{i\theta_4(q, \bar{q})} \Psi_{\{q, \bar{q}\}}(\vec{z}_1, \vec{z}_2, \dots, \vec{z}_4), \\ \mathbb{M} \Psi^\pm(\vec{z}_1, \vec{z}_2, \dots, \vec{z}_4) &\stackrel{\text{def}}{=} \Psi^\pm(\vec{z}_4, \vec{z}_3, \dots, \vec{z}_1) \\ &= \pm \Psi^\pm(\vec{z}_1, \vec{z}_2, \dots, \vec{z}_4). \end{aligned} \quad (20)$$

where  $\pm q = (q_2, \pm q_3, q_4)$  and

$$\Psi^\pm(\vec{z}_1, \vec{z}_2, \dots, \vec{z}_4) = \frac{1}{2} (\Psi_{\{q, \bar{q}\}}(\vec{z}_1, \vec{z}_2, \dots, \vec{z}_4) \pm \Psi_{\{-q, -\bar{q}\}}(\vec{z}_1, \vec{z}_2, \dots, \vec{z}_4)). \quad (21)$$

The eigenvalues of  $\mathbb{P}$  depend on quasimomentum  $\theta_N = 0, \frac{\pi}{2}, \pi, \frac{3\pi}{2}$ . According to the Bose symmetry of the reggeized gluons  $\theta_4 = 0$  [11].

### 2.3. Normalization of the Baxter solution

It turns out that the norm (7) can be also rewritten in terms of eigenvalues of  $\mathbb{Q}(u, \bar{u})$  [10]. The  $\text{SL}(2, \mathbb{C})$  scalar product is normalized as

$$\begin{aligned} \int \Psi_{\vec{p}, \{q, \bar{q}\}}(\vec{z}_1, \vec{z}_2, \vec{z}_3, \vec{z}_4) (\Psi_{\vec{p}', \{q', \bar{q}'\}}(\vec{z}_1, \vec{z}_2, \vec{z}_3, \vec{z}_4))^* \prod_{k=1}^4 d^2 z_k = \\ = (2\pi)^4 \delta^{(2)}(\vec{p} - \vec{p}') \delta_{\{q, \bar{q}\} \{q', \bar{q}'\}}, \end{aligned} \quad (22)$$

where  $q = (q_2, q_3, q_4)$  and anti-holomorphic  $\bar{q} = (\bar{q}_2, \bar{q}_3, \bar{q}_4)$  depend on real  $\nu_h$ , integer  $n_h$  and on the set of integers  $\ell = (\ell_1, \ell_2, \ell_3, \ell_4)$ . The Reggeon wave-function in Sklyanin representation (SoV) [20, 10] can be written using separated coordinates  $\vec{x} = (\vec{x}_1, \vec{x}_2, \vec{x}_3)$  as

$$\begin{aligned} \Psi_{\vec{p}, \{q, \bar{q}\}}(\vec{z}_1, \vec{z}_2, \vec{z}_3, \vec{z}_4) = \\ = \int d^3 \vec{x} \mu(\vec{x}_1, \vec{x}_2, \vec{x}_3) U_{\vec{p}, \vec{x}}(\vec{z}_1, \vec{z}_2, \vec{z}_3, \vec{z}_4) (\Phi_{\{q, \bar{q}\}}(\vec{x}_1, \vec{x}_2, \vec{x}_3))^*, \end{aligned} \quad (23)$$

where  $\vec{x} = (\vec{x}_1, \vec{x}_2, \vec{x}_3)$  are separated variables,  $U_{\vec{p}, \vec{x}}(\vec{z}_1, \dots, \vec{z}_4)$  is unitary transformation while

$$(\Phi_{\{q, \bar{q}\}}(\vec{x}_1, \vec{x}_2, \vec{x}_3))^* = e^{i\theta_4(q, \bar{q})/2} \prod_{k=1}^3 \left( \frac{\bar{x}_k}{x_k} \right)^4 Q_{q, \bar{q}}(x_k, \bar{x}_k), \quad (24)$$

and  $Q_{q, \bar{q}}(x_k, \bar{x}_k)$  is the eigenvalue of the Baxter operator. The separated coordinates

$$x_k = \nu_k - \frac{in_k}{2}, \quad \bar{x}_k = \nu_k + \frac{in_k}{2}, \quad (25)$$

are parameterized by  $n_k$  integer and  $\nu_k$  real<sup>2</sup>. Integration over their space implies

$$\int d^3 \vec{x} = \prod_{k=1}^3 \sum_{n_k=-\infty}^{\infty} \int_{-\infty}^{\infty} d\nu_k, \quad \mu(\vec{x}) = \frac{2}{6\pi^{16}} \prod_{j,k=1, j>k}^3 |\vec{x}_k - \vec{x}_j|^2, \quad (26)$$

where  $|\vec{x}_k - \vec{x}_j|^2 = (\nu_k - \nu_j)^2 + (n_h - n_j)^2/4$ . The unitary integral kernel  $U_{\vec{p}, \vec{x}}$  can be rewritten

$$U_{\vec{p}, \vec{x}}(\vec{z}_1, \dots, \vec{z}_4) = c_4(\vec{x}) (\vec{p}^2)^{3/2} \int d^2 z_0 e^{2i\vec{p} \cdot \vec{z}_0} U_{\vec{x}}(\vec{z}_1, \dots, \vec{z}_4; \vec{z}_0), \quad (27)$$

---

<sup>2</sup> The parameters  $n_k$  and  $\nu_k$  should not be identified with  $n_h$  and  $\nu_h$  from Eq. (16).

with  $2\vec{p} \cdot \vec{z}_0 = p z_0 + \bar{p} \bar{z}_0$  and it is normalized to

$$\begin{aligned} \int d^4 \vec{z} U_{\vec{p}, \vec{x}}(\vec{z}_1, \dots, \vec{z}_4) \left( U_{\vec{p}', \vec{x}'}(\vec{z}_1, \dots, \vec{z}_4) \right)^* = \\ = (2\pi)^4 \delta^{(2)}(\vec{p} - \vec{p}') \{ \delta(\vec{x} - \vec{x}') + \dots \} \frac{1}{6\mu(\vec{x})}, \end{aligned} \quad (28)$$

where  $\vec{z} = (\vec{z}_1, \dots, \vec{z}_4)$  and ellipses denote the sum of terms involving all permutations of the vector inside the  $\vec{x} = (\vec{x}_1, \vec{x}_2, \vec{x}_3)$ . The kernel  $U_{\vec{x}}$  is defined in Ref. [10]. Substituting the above formulae, the scalar product of the eigenstates (22) is given by

$$\begin{aligned} (2\pi)^4 \delta^{(2)}(\vec{p} - \vec{p}') e^{i(\theta_4(q, \bar{q}) - \theta_4(q', \bar{q}'))/2} \int \prod_{k=1}^3 d^2 x_k^* (\mu(\vec{x}_1, \vec{x}_2, \vec{x}_3))^* \\ \times Q_{q, \bar{q}}(x_k, \bar{x}_k) (Q_{q', \bar{q}'}(x_k, \bar{x}_k))^* = (2\pi)^4 \delta^{(2)}(\vec{p} - \vec{p}') \delta_{\{q, \bar{q}\} \{q', \bar{q}'\}}. \end{aligned} \quad (29)$$

where  $d^2 x_k^* (\mu(\vec{x}_1, \vec{x}_2, \vec{x}_3))^* = d^2 x_k \mu(\vec{x}_1, \vec{x}_2, \vec{x}_3)$  and  $\delta_{\{q, \bar{q}\} \{q', \bar{q}'\}} = \delta(\nu_h - \nu'_h) \delta_{n_h n'_h} \delta_{\ell \ell'}$ . The quasimomentum  $\theta_4$  depends only on integer parameters, *i.e.*  $n_h, \ell$ , therefore for the orthonormal states the normalization condition can be written up to the momentum term as

$$\begin{aligned} \langle q, \bar{q} | q', \bar{q}' \rangle \stackrel{\text{def}}{=} (2\pi)^4 \int \prod_{k=1}^3 d^2 x_k \mu(\{\vec{x}_k\}) Q_{q, \bar{q}}(x_k, \bar{x}_k) (Q_{q', \bar{q}'}(x_k, \bar{x}_k))^* = \\ = (2\pi)^4 \delta(\nu_h - \nu'_h) \delta_{n_h n'_h} \delta_{\ell \ell'}, \end{aligned} \quad (30)$$

with  $|q, \bar{q}\rangle$  being a product of the Baxter equation eigenstates.

### 3. Baxter differential equation

Substituting the following integral ansatz [11]

$$Q_{q, \bar{q}}(u, \bar{u}) = \int \frac{d^2 z}{z \bar{z}} z^{-iu} \bar{z}^{-i\bar{u}} \tilde{Q}_{q, \bar{q}}(z, \bar{z}), \quad (31)$$

to Baxter equations (10)-(11) where we integrate over the two-dimensional  $\vec{z}$ -plane with  $\bar{z} = z^*$  and  $\tilde{Q}_{q, \bar{q}}(z, \bar{z})$  depends on  $\{q, \bar{q}\}$  one obtains the fourth order differential equation for the function  $\tilde{Q}_{q, \bar{q}}(z, \bar{z})$

$$\left[ z^s (z \partial_z)^4 z^{1-s} + z^{-s} (z \partial_z)^4 z^{s-1} - 2(z \partial_z)^4 - \sum_{k=2}^4 i^k q_k (z \partial_z)^{4-k} \right] \tilde{Q}_{q, \bar{q}}(z, \bar{z}) = 0. \quad (32)$$



A similar equation holds in the anti-holomorphic sector with  $s$  and  $q_k$  replaced by  $\bar{s} = 1 - s^*$  and  $\bar{q}_k = q_k^*$ , respectively. Conditions for the analytical properties and asymptotic behaviour of  $Q_{q,\bar{q}}(u, \bar{u})$  become equivalent to a requirement for  $\tilde{Q}_{q,\bar{q}}(z, \bar{z} = z^*)$  to be a single-valued function on the complex  $z$ -plane. The differential equation (32) possesses three regular singular points located at  $z = 0$ ,  $z = 1$  and  $z = \infty$ . Around each of this points one can construct four linearly independent solutions,  $Q_a(z)$ . Similar relations hold for the anti-holomorphic equation with four independent solutions being  $\bar{Q}_b(\bar{z})$ .

The general expression for the Baxter function reads then:

$$\tilde{Q}_{q,\bar{q}}(z, \bar{z}) = \sum_{a,b=1}^4 Q_a(z) C_{ab} \bar{Q}_b(\bar{z}), \quad (33)$$

where  $C_{ab}$  is a mixing matrix. The functions  $Q_a(z)$  and  $\bar{Q}_b(\bar{z})$  have a non-trivial monodromy<sup>3</sup> around three singular points,  $z, \bar{z} = 0, 1$  and  $\infty$ . In order to be well-defined on the whole plane, functions  $\tilde{Q}_{q,\bar{q}}(z, \bar{z} = z^*)$  should be single-valued and their monodromy should cancel in the r.h.s. of Eq. (33). This requirement determines the values of the mixing coefficients,  $C_{ab}$ , and also allows to calculate the quantized values of the conformal charges  $q_k$ .

It turns out that the differential equation (32) is also symmetric under the transformation  $z \rightarrow 1/z$  with  $q_k \rightarrow (-1)^k q_k$ . This property leads to

$$\tilde{Q}_{q,\bar{q}}(z, \bar{z}) = e^{i\theta_4(q,\bar{q})} \tilde{Q}_{-q,-\bar{q}}(1/z, 1/\bar{z}), \quad (34)$$

where  $\pm q = (q_2, \pm q_3, q_4)$  denotes the integrals of motion corresponding to the function  $\tilde{Q}_{q,\bar{q}}(z, \bar{z})$ . The above formula allows us to define the solution  $\tilde{Q}_{q,\bar{q}}(z, \bar{z})$  around  $z = \infty$  from the solution at  $z = 0$ . Thus, applying (34) we are able to find  $\tilde{Q}_{q,\bar{q}}(z, \bar{z})$  and analytically continue it to the whole  $z$ -plane.

### 3.1. Solution around $z = 0$

Solutions  $Q(z) \sim z^a$  around  $z = 0$  can be found by the series method. The indicial equation for the solutions of Eq. (32) reads as follows

$$(a - 1 + s)^4 = 0. \quad (35)$$

---

<sup>3</sup> The monodromy matrix around  $z = 0$  is defined as  $Q_n^{(0)}(ze^{2\pi i}) = M_{nk} Q_k^{(0)}(z)$  and similarly for the other singular points.

with four-times degenerate  $a = 1 - s$ . Therefore, the fundamental set of linearly independent solutions to (32) around  $z = 0$  is given by

$$Q_m^{(0)}(z) = z^{1-s} \sum_{k=0}^{m-1} \frac{(m-1)!}{k!(m-k-1)!} u_{k+1}(z) \text{Log}^{m-k-1}(z), \quad (36)$$

with  $1 \leq m \leq 4$ . The functions

$$u_m(z) = 1 + \sum_{n=1}^{\infty} z^n u_n^{(m)}(q). \quad (37)$$

are defined inside the region  $|z| < 1$ . Inserting (36) and (37) into (32), one derives recurrence relations for  $u_n^{(m)}(q)$ . Their explicit form can be found in the Appendix A.1.

The general solution for  $\tilde{Q}_{q,\bar{q}}(z, \bar{z})$  around  $z = 0$  can be obtained gluing holomorphic and anti-holomorphic sectors

$$\tilde{Q}(z, \bar{z})_{q,\bar{q}} \stackrel{|z| \rightarrow 0}{=} \sum_{m,\bar{m}=1}^4 Q_m^{(0)}(z) C_{m\bar{m}}^{(0)} \bar{Q}_{\bar{m}}^{(0)}(\bar{z}). \quad (38)$$

where the fundamental set of solutions in the anti-holomorphic sector can be obtained from (36) by substituting  $s$  and  $q_k$  by  $\bar{s} = 1 - s^*$  and  $\bar{q}_k = q_k^*$ , respectively. The above solution (38) should be single-valued on the  $z$ -plane. This implies that the mixing matrix  $C_{m\bar{m}}^{(0)}$  for  $n + m \leq 5$  has the following structure

$$C_{nm}^{(0)} = \frac{\sigma}{(n-1)!(m-1)!} \sum_{k=0}^{4-n-m+1} \frac{(-2)^k}{k!} \alpha_{k+n+m-1} \quad (39)$$

with  $\sigma, \alpha_1, \alpha_2, \alpha_3$  being arbitrary complex parameters and  $\alpha_4 = 1$ . Below the main anti-diagonal, that is for  $n + m > 4 + 1$ ,  $C_{nm}^{(0)}$  vanish.

Using the above formulae one can derive from (18) an expression for the energy

$$E_4(q, \bar{q}) = \text{Re} \left[ \frac{\alpha_3(-q, -\bar{q})}{\alpha_4(-q, -\bar{q})} + \frac{\alpha_3(q, \bar{q})}{\alpha_4(q, \bar{q})} \right], \quad (40)$$

where the arbitrary complex parameters  $\alpha_3$  and  $\alpha_4$ , defined in Eq. (39), will be fixed by the quantization conditions.

### 3.2. Solution around $z = 1$

Solving Eq. (32) around  $z = 1$  with asymptotics  $Q(z) \sim (z - 1)^b$  we obtain the following indicial equation

$$(b + 1 + h - 4s)(b + 2 - h - 4s)(b - 1)b = 0, \quad (41)$$

where  $h$  is the total  $\text{SL}(2, \mathbb{C})$  spin defined by (16). Although the solutions  $b = 0, 1$  differ by an integer, for  $h \neq (1 + n_h)/2$ , one can construct four solutions  $Q_i^{(1)}(z)$  without logarithmic terms. The  $\text{Log}(1 - z)$ -terms are only needed for  $\text{Im}[h] = 0$  where additional degeneration occurs. The solutions with  $\text{Im}[h] \neq 0$  will be constructed in Section 4 while the ones with  $\text{Im}[h] = 0$  in Sections 5 and 6.

Let us consider the duality relation (34). Using the function  $\tilde{Q}_{q, \bar{q}}(z, \bar{z})$  we evaluate

$$\tilde{Q}_{q, \bar{q}}(z, \bar{z}) \stackrel{|z| \rightarrow 1}{=} \sum_{m, \bar{m}=1}^4 Q_m^{(1)}(z) C_{m\bar{m}}^{(1)} \overline{Q}_{\bar{m}}^{(1)}(\bar{z}). \quad (42)$$

in the limit  $|z| \rightarrow 1$ . In this way we obtain a set of relations for the functions  $C_{m\bar{m}}^{(1)}(q, \bar{q})$ . The derivation is based on the following property

$$Q_a^{(1)}(1/z; -q) = \sum_{b=1}^4 S_{ab} Q_b^{(1)}(z; q), \quad (43)$$

with  $\text{Im}[1/z] > 0$  and where the dependence on the integrals of motion was explicitly indicated. Here taking  $z \rightarrow 1$  limit in (42) and substituting to (43) we are able to evaluate the  $S$ -matrix. Similar relations hold in the anti-holomorphic sector. The  $S$ -matrix does not depend on  $z$  because the  $Q$ -functions on both sides of relation (43) satisfy the same differential equation (32).

Now, substituting (42) and (43) into (34), we find

$$C_{m\bar{m}}^{(1)}(q, \bar{q}) = e^{i\theta_4(q, \bar{q})} \sum_{n, \bar{n}=1}^4 S_{nm} C_{n\bar{n}}^{(1)}(-q, -\bar{q}) \overline{S}_{\bar{n}\bar{m}}. \quad (44)$$

Using the mixing matrix at  $z = 1$  we can compute from Eq. (44), the eigenvalues of the quasimomentum,  $\theta_4(q, \bar{q})$ .

### 3.3. Transition matrices

In the previous sections we discussed the solutions  $\tilde{Q}_{q, \bar{q}}(z, \bar{z})$  to (32) in the vicinity of  $z = 0$  and  $z = 1$ . In order to calculate  $\tilde{Q}_{q, \bar{q}}(z, \bar{z})$  on the whole complex  $z$ -plane one can glue these solutions in the region  $|1 - z| < 1$ ,  $|z| < 1$

and, then analytically continue the resulting expression for  $\tilde{Q}_{q,\bar{q}}(z, \bar{z})$  by making use of the duality relation (34).

To this end, we define the transition matrices  $\Omega(q)$  and  $\bar{\Omega}(\bar{q})$ :

$$Q_n^{(0)}(z) = \sum_{m=1}^4 \Omega_{nm}(q) Q_m^{(1)}(z), \quad \bar{Q}_n^{(0)}(\bar{z}) = \sum_{m=1}^4 \bar{\Omega}_{nm}(\bar{q}) \bar{Q}_m^{(1)}(\bar{z}). \quad (45)$$

which are uniquely fixed [11] and do not depend on  $z$  and  $\bar{z}$ . Substituting (45) into (38) and matching the result into (42), we find the following relation

$$C^{(1)}(q, \bar{q}) = [\Omega(q)]^T C^{(0)}(q, \bar{q}) \bar{\Omega}(\bar{q}). \quad (46)$$

The above matrix formula contains 16 complex equations with: three  $\alpha$ -parameters inside the matrix  $C^{(0)}$ , six parameters<sup>4</sup> inside the matrix  $C^{(1)}$ , two integrals of motion  $q_3, q_4$  with  $\bar{q}_k = q_k^*$ , where  $q_2 = q_2^*$  has been already quantized (16). Thus, one obtains five nontrivial consistency conditions. Next, Eq. (46) allows us to determine the matrices  $C^{(0)}$  and  $C^{(1)}$  and provides the quantization conditions for the integrals of motion,  $q_k$  and  $\bar{q}_k$  with  $k = 3, 4$ . The numerical solutions [21] to the quantization conditions (46) will be presented in details in the next sections. Finally, using these quantized conformal charges one can evaluate the eigenvalues of the Baxter  $\mathbb{Q}$ -operator (31) and the Hamiltonian eigenvalues (40).

### 3.4. Norm with integral ansatz

Substituting the ansatz (31) to (30) we can also rewrite the norm in terms of  $\tilde{Q}_{q,\bar{q}}(z, \bar{z})$  solutions. To evaluate this norm we use the following correspondence

$$x Q_{q,\bar{q}}(x, \bar{x}) = -i \int d^2 z \, z^{-ix-1} \bar{z}^{-i\bar{x}-1} z \partial_z \tilde{Q}_{q,\bar{q}}(z, \bar{z}),$$

with  $n = x - \bar{x}$ ,  $2\lambda = x + \bar{x}$  and

$$\int_{-\infty}^{\infty} d\lambda \sum_{n=-\infty}^{\infty} z^{-ix} \bar{z}^{-i\bar{x}} w^{ix} \bar{w}^{i\bar{x}} = 2\pi^2 z \bar{z} \delta^{(2)}(z - w). \quad (47)$$

---

<sup>4</sup> Here, this number is taken for ordinary solutions but it depends on values of conformal charges and will be calculated in the next sections.

The final expression for the scalar product defined in (29) reads as

$$\begin{aligned} \langle q, \bar{q} | q', \bar{q}' \rangle = \frac{4^4}{6\pi^6} \left( \prod_{k=1}^3 \frac{d^2 z_k}{z_k \bar{z}_k} \right) & \left( \tilde{Q}_{q', \bar{q}'}(z_1, \bar{z}_1) \dots \tilde{Q}_{q', \bar{q}'}(z_3, \bar{z}_3) \right)^* \\ & \times \left( \prod_{1 \leq i < j}^3 (-D_{ij} \bar{D}_{ij}) \right) \tilde{Q}_{q, \bar{q}}(z_1, \bar{z}_1) \dots \tilde{Q}_{q, \bar{q}}(z_3, \bar{z}_3), \quad (48) \end{aligned}$$

where  $D_{ij} = z_i \partial_i - z_j \partial_j$ . In this work the above expression is used to test the normalization condition.

#### 4. Trajectory-like solutions and their analytical continuation

In this section we parameterize possible values of conformal charges with use of WKB approximation. Next, we construct trajectory-like solutions with  $\nu_h \in \mathbb{R}$  and perform their analytical continuation into  $\nu_h \in \mathbb{C}$  that allows to explain the existence of specific point-like solutions with  $\nu_h = 0$ .

##### 4.1. WKB approximation

Finding asymptotic solutions [12] to the Baxter equations, (10) and (11), one can derive the WKB approximation of the conformal charges  $q_3$  and  $q_4$ .

In the limit of large values of conformal charges, *i.e.* where  $q_4^{1/4} \gg q_3^{1/3} \gg q_2^{1/2}$

$$q_4^{1/4} = \frac{\Gamma^2(3/4)}{4\sqrt{\pi}} \left[ \frac{1}{\sqrt{2}} \ell_1 + \frac{i}{\sqrt{2}} \ell_2 \right]. \quad (49)$$

Thus, for fixed  $q_2$  and  $q_3$  the quantized values of  $q_4^{1/4}$  can be identified with  $(\ell_1, \ell_2)$ -vertices of square-like WKB lattices. One can see an example of such a correspondence in Fig. 4. In the following the  $q_k$ -spectrum related to vertices of WKB lattice will be called lattice spectrum or  $q_k$ -lattice.

The next two integers,  $\ell_3$  and  $\ell_4$ , establish dependence between values of  $q_4$  and  $q_3$  [14, 13]. The leading approximation for the charge  $q_3$  reads

$$\text{Im} \left[ \frac{q_3}{q_4^{1/2}} \right] = \ell_3, \quad (50)$$

where  $\ell_3$  describes a “twist” between  $q_4^{1/4}$  and  $q_3^{1/2}$  WKB lattices. For  $\ell_3 = 0$  one obtains resemblant lattices without any “twist”. An example of such spectrum is plotted in Fig. 5 where the  $q_4^{1/4}$ -lattice has similar structure to

the  $q_3^{1/2}$ -lattice. For  $\ell_3 \neq 0$   $q_4^{1/4}$ -lattice winds faster than corresponding  $q_3^{1/2}$ -lattice. This situation is presented in Fig. 6.

The system of Eqs. (49) and (50) is underdetermined and it does not fix the charge  $q_3$  completely. The last parameter,  $\ell_4$ , describes the scale between  $q_4^{1/4}$  and  $q_3^{1/2}$  WKB lattices but its exact analytical relation to conformal charges even in the WKB approximation is unknown.

The quasimomentum in the WKB approximation reads as follows

$$\theta_4 = -\frac{\pi}{2}\ell_\theta = \frac{\pi}{2}(\ell_2 + \ell_3 - \ell_1) \pmod{2\pi}, \quad (51)$$

where  $\ell_1, \ell_2$  and  $\ell_3$  are even for even  $\ell_\theta$  and odd for odd  $\ell_\theta$ . Thus, we have two kinds of lattices: with  $\theta_4 = 0, \pi$  and with  $\theta_4 = \pi/2, 3\pi/2$ . Therefore, for a given lattice not all vertices are occupied.

The last conformal charge,  $q_2 = -h(h-1)$ , depends on  $n_h$  and  $\nu_h$  (16). Since,  $\nu_h$  is real and continuous the conformal charges form one dimensional trajectories. One can see an example of the trajectories in Figs. 1 and 2. The WKB approximation applies for large values of conformal charges therefore our exact numerical results agree better with WKB for  $q_4 \rightarrow \infty$ . When  $q_4$  goes to zero the approximation stops to work. The numerical results from Ref. [13] and from the present paper show lack of quantized values of  $q_4^{1/4}$  in the centre of the lattice, for example in Fig. 4.

#### 4.2. Solution around $z = 1$ for $\text{Im}[h] \neq 0$

In this Section we briefly recapitulate the method to solve Eq. (32) exactly. For  $\nu_h \neq 0$  and  $n_h > 0$  we define around  $z = 1$  the following fundamental set of solutions<sup>5</sup>

$$\begin{aligned} Q_m^{(1)}(z) &= z^{1-s}(1-z)^{m-1}v_m(z), \\ Q_3^{(1)}(z) &= z^{1-s}(1-z)^{4s-h-1}v_3(z), \\ Q_4^{(1)}(z) &= z^{1-s}(1-z)^{4s+h-2}v_4(z), \end{aligned} \quad (52)$$

where  $m = 1, 2$ . The functions  $v_k(z)$  are given by the power series

$$v_k(z) = \sum_{n=0}^{\infty} (1-z)^n v_n^{(k)}(q), \quad (53)$$

which converge inside the region  $|1-z| < 1$  and where the expansion coefficients  $v_n^{(k)}$  satisfy the four-term recurrence relations<sup>6</sup> with respect to the

<sup>5</sup> Exchange  $n_h \rightarrow -n_h$  corresponds to  $Q_3^{(1)}(z) \leftrightarrow Q_4^{(1)}(z)$

<sup>6</sup> The factor  $z^{1-s}$  was included in the r.h.s. of (52) to simplify the form of the recurrence relations.

index  $n$ . Their explicit form can be found in the Appendix A.2. Similar calculations have to be performed in the anti-holomorphic sector with  $s$  and  $h$  replaced by  $\bar{s} = 1 - s^*$  and  $\bar{h} = 1 - h^*$ , respectively.

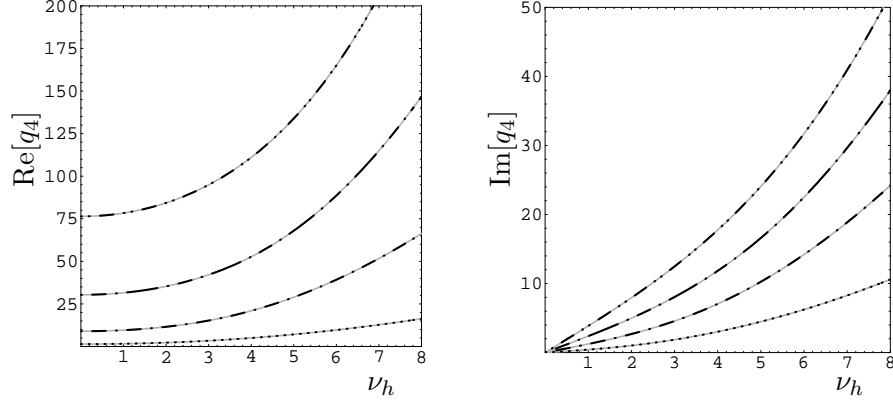


Figure 1. Trajectories of conformal charges for  $q_3 = 0$  and  $h = \frac{3}{2} + i\nu_h$  where  $\nu_h \in \mathbb{R}$

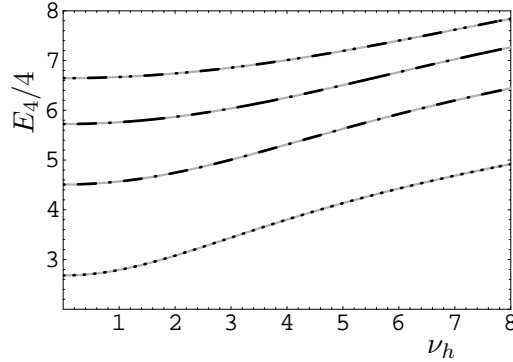


Figure 2. The energy along the trajectories from Fig. 1 as a function of  $\nu_h$

A general solution for  $\tilde{Q}_{q,\bar{q}}(z, \bar{z})$  for  $\text{Im}[h] \neq 0$  that satisfies the single-valuedness condition can be constructed as

$$\tilde{Q}_{q,\bar{q}}(z, \bar{z}) \stackrel{|z| \rightarrow 1}{=} \beta_h Q_4^{(1)}(z) \bar{Q}_4^{(1)}(\bar{z}) + \beta_{1-h} Q_3^{(1)}(z) \bar{Q}_3^{(1)}(\bar{z}) + \sum_{m, \bar{m}=1}^2 Q_m^{(1)}(z) C_{m\bar{m}}^{(1)} \bar{Q}_{\bar{m}}^{(1)}(\bar{z}). \quad (54)$$

Here the parameters  $\beta_h = C_{44}^{(1)}$  while  $\beta_{1-h} = C_{33}^{(1)}$ . The  $\beta$ -coefficients depend, in general, on the total spin  $h$  and  $\bar{h} = 1 - h^*$ . They are chosen in such a way that the symmetry of the eigenvalues of the Baxter operator under  $h \rightarrow 1 - h$  becomes manifest. Thus, the mixing matrix  $C^{(1)}$  defined in (54) depends on  $2 + 2^2$  complex parameters  $\beta_h$ ,  $\beta_{1-h}$  and  $C_{m\bar{m}}^{(1)}$  which

are functions of the integrals of motion  $(q, \bar{q})$ , so they can be fixed by the quantization conditions.

The functions defined by Eqs. (52) and (36) give the solutions  $\tilde{Q}_{q, \bar{q}}(z, \bar{z})$ . Their conformal charges calculated from Eq. (46) form in the  $q_k$ -space continuous trajectories propagating in the  $\nu_h$ -real space. An example of such trajectories for  $q_3 = 0$  and  $h = \frac{3}{2} + i\nu_h$  where  $\nu_h \in \mathbb{R}$  is plotted in Fig. 1. We can also calculate the energy along the trajectories, Fig. 2. However, for  $\nu_h = 0$  solutions to Eq. (32) have a different form. Therefore, one has to consider these solutions separately. We will discuss them in the next sections.

#### 4.3. Analytical continuation

Let us consider analytical continuation of  $E_4(\nu_h)$  into the complex  $\nu_h$ -plane, the same as the one performed in calculation of anomalous dimensions in deep inelastic scattering processes [5]. The requirement for  $n_h$  to be integer follows from condition for singlevaluedness of the wave-function  $\Psi_{\vec{p}, \{q, \bar{q}\}}$ . On the other hand  $\Psi_{\vec{p}, \{q, \bar{q}\}}$  is normalizable with the respect to Eq. (7) when  $\nu_h$  is real. Therefore performing analytical continuation we relax the normalization condition (30) while keeping the quantization conditions (46). This in turn implies that the operator of Hermitian conjugation, which is related to the scalar product, is not well defined. It follows that:

$$h^* \neq 1 - \bar{h}, \quad q_k^* \neq \bar{q}_k. \quad (55)$$

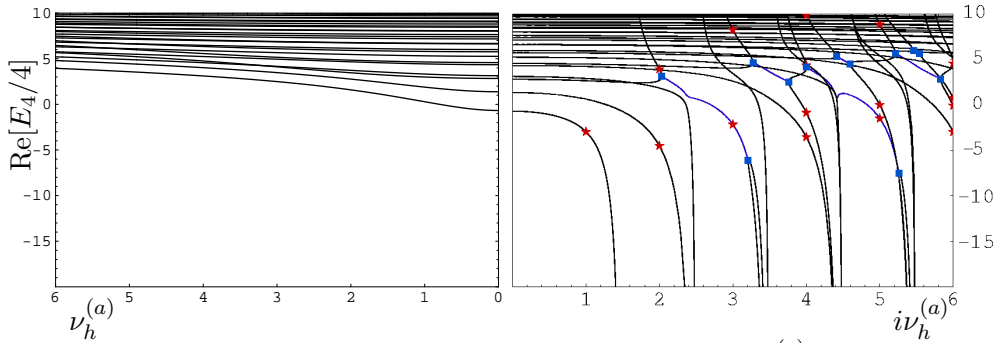


Figure 3. Energy and its analytical continuation in  $h^{(a)} = \frac{1}{2} + i\nu_h^{(a)} \in \mathbb{R}$  direction. Here, *stars* are related to the twin-solutions of the point-like solutions with  $n_h^{(p)} \in 2\mathbb{Z}$ . For  $q_3 = 0$  and  $n_h^{(p)} \in 2\mathbb{Z} + 1$  we have only point-like solutions. Trajectories between branching points (*boxes*) have non-vanishing imaginary part of  $E_4$  and  $q_4 = \bar{q}_4$ .

One can notice that in the analytical continuation region there is a trans-



formation

$$(h, \bar{h}) \rightarrow (h, 1 - \bar{h}), \quad (56)$$

which does not change the values of Casimirs (15) and the quantization conditions are also invariant under this transformation<sup>7</sup>. The symmetry (56) relates two different solutions from analytically continued sheets which have the same conformal charges but different conformal weights, *i.e.*  $h^{(p)}$  and  $h^{(a)}$ . Requirements  $h^{(p)} = h^{(a)}$  and  $\bar{h}^{(p)} = 1 - \bar{h}^{(a)}$  give conditions

$$\text{Re}[\nu_h^{(a)}] = \text{Re}[\nu_h^{(p)}] = 0, \quad n_h^{(a)} = -2\text{Im}[\nu_h^{(p)}], \quad n_h^{(p)} = -2\text{Im}[\nu_h^{(a)}]. \quad (57)$$

Since conformal Lorentz spins are integer, the symmetry (56) exists only for half-integer and integer conformal weights. Now, if  $h^{(p)}$  has  $\nu_h^{(p)} \in \mathbb{R}$  and another one,  $h^{(a)}$ , from analytical continuation region has  $\nu_h^{(a)} \in \mathbb{C}$  then Eq. (57) implies that  $n_h^{(a)} = 0$ ,  $\nu_h^{(p)} = 0$  and  $n_h^{(p)} = 2i\nu_h^{(a)}$ . Thus, all solutions with  $h^{(a)} = \bar{h}^{(a)} = \frac{1}{2} + i\nu_h^{(a)} \in \mathbb{Z}/2$ , *i.e.* situated on analytical continuation (Riemann) surfaces of  $n_h^{(a)} = 0$  physical states, have their twin-solutions with  $h^{(p)} = \frac{1+n_h^{(p)}}{2}$ ,  $\bar{h}^{(p)} = \frac{1-n_h^{(p)}}{2} \in \mathbb{Z}/2$ , where  $n_h^{(p)}/2 = i\nu_h^{(a)}$ . The symmetry (56) can move the twin-solutions outside the physical region therefore solutions denoted by  $(p)$  can be either normalizable or non-normalizable.

Let us focus on the set of solutions with  $q_4 = \bar{q}_4$  and  $q_3 = \bar{q}_3 = 0$ . On the left panel of Fig. 3 energy of such trajectories with  $n_h = 0$  and  $\nu_h \in \mathbb{R}$  is plotted. Relaxing the normalization condition (7) we perform analytical continuation of this energy plot to complex  $\nu_h$ -plane. The energies as functions of  $\nu_h \in \mathbb{C}$  form complicated Riemann surfaces. One can see their cross-section in  $i\nu_h \in \mathbb{R}$  direction on the right panel of Fig. 3. For example, due to the symmetry (56) and the conditions (57), the solutions for  $i\nu_h^{(a)} = 1$  should have twin-solutions with  $n_h^{(p)} = 2$  and  $\nu_h^{(p)} = 0$ . Performing numerical calculation one can find physical trajectories for all solutions with  $h^{(p)} = \frac{3}{2} + i\nu_h^{(p)}$ , *e.g.* the ones from Figs. 1 and 2, except the twin-solution to the solution with  $i\nu_h^{(a)} = 1$  denoted in Fig. 3 by *star*. It means that the latter twin-solution is not situated on any trajectory, *i.e.* it is a point-like solution. Other similar point-like twin-solutions without physical trajectories exist to all solutions denoted in this figure by *stars*. Moreover, since there is not any trajectory for  $q_4 = \bar{q}_4$  and  $q_3 = \bar{q}_3 = 0$  all solutions with  $i\nu_h \in \frac{2\mathbb{Z}+1}{2}$  from the right panel of Fig. 3 have their point-like twin-solutions.

The point-like solutions are candidates for Hamiltonian eigenstates (6) with discrete spectrum. The point-like states do not depend on continuous

---

<sup>7</sup> Due to the symmetry of the spectrum  $(h, \bar{h}) \rightarrow (1-h, 1-\bar{h})$ , we have also a transformation  $(h, \bar{h}) \rightarrow (1-h, \bar{h})$ , which is analogical to (56).

parameter  $\nu_h$ . In order to contribute to the decomposition of the Hamiltonian over the eigenstates, their scalar product (48) should be proportional to  $\delta_{n_h n'_h} \delta_{\ell \ell'}$  without  $\delta(\nu_h - \nu'_h)$ . On the other hand the eigenstates should properly transform with respect to  $SL(2, \mathbb{C})$  group. This implies that the scalar product (48) should be infinite or equal to zero. Thus, one may suppose that the point-like solutions are non-normalizable with respect to the  $SL(2, \mathbb{C})$  scalar product (7). In the next sections we present properties and check normalizability of the solutions with half-integer and integer conformal weights in more detail.

### 5. Solution from the trajectories with $\nu_h = 0$

Let us consider an ordinary solution<sup>8</sup> to Eq. (32) around  $z = 1$  with  $\nu_h = 0$ . Conformal charges of these ordinary solutions are situated on  $q_k$ -trajectories propagating in continuous  $\nu_h$ . Thus, these solutions should be normalized to Dirac delta function. Indeed, one can find by explicit calculation that their scalar product is proportional to  $\delta(\nu_h - \nu'_h)$ . In this section we are going to describe construction of the ordinary solutions whose conformal charges form resemblant, winding and descendent lattices (49)-(50).

#### 5.1. Trajectory-like solutions around $z = 1$ for even $n_h$

Solving Baxter differential equations with  $n_h \in 2\mathbb{Z}_+$  and  $\nu_h = 0$  one constructs

$$Q_i^{(1)}(z) = z^{1-s} v_i(1-z), \quad (58)$$

where

$$\begin{aligned} v_m(y) &= y^{b_m} \sum_{n=0}^{\infty} v_n^{(m)} y^n, \\ v_4(y) &= y^{b_4} \sum_{n=0}^{\infty} v_n^{(4)} y^n + \text{Log}(y) v_2(y), \end{aligned} \quad (59)$$

with  $m = 1, 2, 3$  and  $b_1 = 1$ ,  $b_2 = 0$ ,  $b_3 = h - 2 + 4s$ ,  $b_4 = -h - 1 + 4s$ . The coefficients  $v_k$  satisfy the four-term recurrence relations with the boundary condition  $v_{n_h} = 1$ . Similar solutions can be found in the anti-holomorphic sector.

---

<sup>8</sup> A solution which has a common structure for almost all values of conformal charges. Contrary to this case, for special values of conformal charges there are other special solutions with smaller number of  $\text{Log}(1-z)$ -terms.

Constructing the general solution (42) for  $h = (1 + n_h)/2$  the two terms on the r.h.s. of (54) look differently in virtue of (59)

$$\tilde{Q}_{q,\bar{q}}(z, \bar{z}) = \beta_1 \left[ Q_4^{(1)}(z) \bar{Q}_3^{(1)}(\bar{z}) + Q_3^{(1)}(z) \bar{Q}_4^{(1)}(\bar{z}) \right] + \beta_2 Q_3^{(1)}(z) \bar{Q}_3^{(1)}(\bar{z}) + \dots, \quad (60)$$

where ellipses denote the remaining terms. Substituting (54) into (31) and performing integration over the region of  $|1 - z| \ll 1$ , one can find the asymptotic behaviour of  $Q(u, \bar{u})$  at large  $u$ .

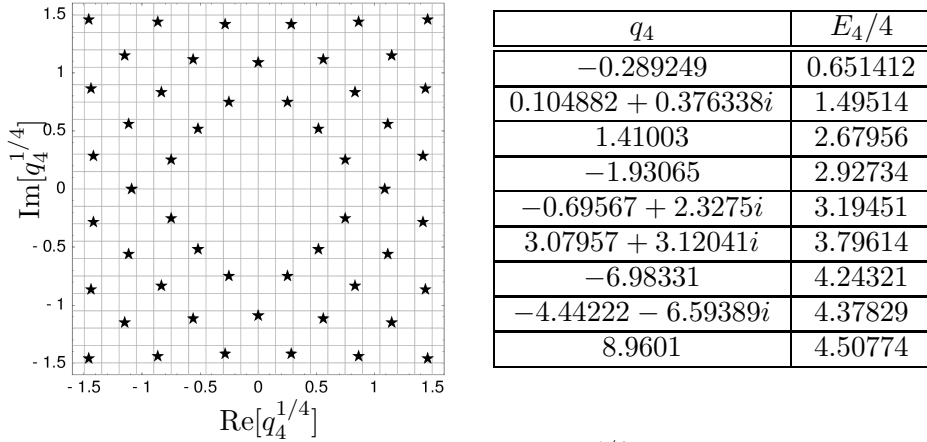


Figure 4. The numerical spectrum of quantized  $q_4^{1/4}$  for trajectory-like solutions with  $n_h = 2$  and  $q_3 = 0$  denoted by stars on the background of the WKB lattice. According to Eq. (50) and Eq. (51) only some vertices of WKB lattice are occupied.

Finally, solving the quantization conditions (46) one can find that conformal charges of (58) are situated on continuous trajectories. Spectrum of conformal charges for  $n_h = 0$  in Refs. [14, 13] as well as  $n_h \neq 0$  can be described by WKB approximation (49)-(51) where parameters  $\ell_i$  with  $i = 1, \dots, 4$  enumerate vertices of WKB lattices. For example in Fig. 4 one can see such lattice spectrum with  $q_3 = 0$  and  $\nu_h = 0$  whose continuation in  $\nu_h \in \mathbb{R}$  form trajectories depicted in Fig. 1. It turns out that the solutions with the lowest energy belong to the  $n_h = 0$  sector [22]. All other states, also those with  $n_h \neq 0$ , have larger energy.

### 5.2. Trajectory-like solutions around $z = 1$ for odd $n_h$

Since for the ordinary solutions with  $h = (1 + n_h)/2 \in \mathbb{Z}$ , i.e.  $n_h$  odd, all roots of Eq. (41) are integer we have two additional terms:  $\text{Log}(1 - z)$  and  $\text{Log}^2(1 - z)$ . Here, the conformal charges form similar lattice structures to the previous  $n_h$  even case. The states also are situated on trajectories with

$\nu_h \neq 0$  defined by Eq. (52). For instance in the  $(h, \bar{h}) = (1, 0)$  sector with  $q_3 \neq 0$  these solutions have a form  $Q_i^{(1)}(z) = z^{1-s} v_i(1-z)$  where

$$\begin{aligned} v_m(y) &= y^{b_m} \sum_{n=0}^{\infty} v_n^{(m)} y^n, \\ v_3(y) &= y^{b_3} \sum_{n=0}^{\infty} v_n^{(3)} y^n + \text{Log}(y) v_2(y), \\ v_4(y) &= y^{b_4} \sum_{n=0}^{\infty} v_n^{(4)} y^n + 2\text{Log}(y) y^{b_3} \sum_{n=0}^{\infty} v_n^{(3)} y^n + \text{Log}^2(y) v_2(y), \end{aligned} \quad (61)$$

while  $m = 1, 2$  and  $b_1 = 1, b_2 = 0, b_3 = -1, b_4 = -2$  for  $s = 0$  and  $b_1 = 0, b_2 = 3, b_3 = 2, b_4 = 1$  for  $s = 1$ .

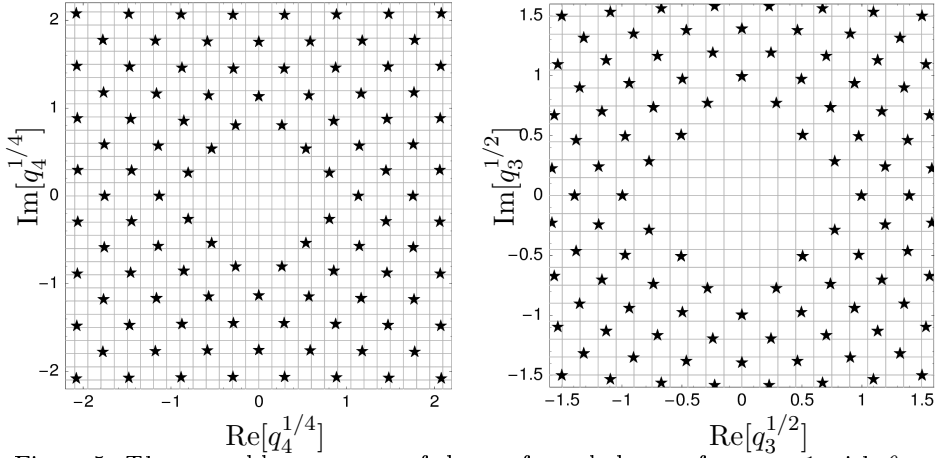


Figure 5. The ressemblant spectra of the conformal charges for  $n_h = 1$  with  $\theta_4 = 0$ . On the left panel the spectrum of  $q_4^{1/4}$ , while on the right panel the spectrum of  $q_3^{1/2}$ .

Fig. 5 with Table 1 show an example of ressemblant lattices where  $\ell_3 = 0$  for  $h = 1$ . We have an infinite number of such lattices and they can be enumerated by an approximate ratio  $|q_4^{1/4}/q_3^{1/2}|$  labelled by  $\ell_4$ . On the other hand in Fig. 6 and Table 2 a part of a winding lattice for  $h = 1$  is presented. These lattices are defined on a complicated winding Riemann surface which has an infinite number of planes enumerated by  $\ell_4$ . We have an infinite number of such lattices labelled by  $\ell_3 \neq 0$ .

It turns out that for  $n_h$  odd and  $q_3 = 0$  trajectory-like solutions do not exist. On the other hand, assuming that the ground state should not

$q_3$	$q_4$	$E_4/4$
$0.512164i$	$-0.332886$	1.10034
$-0.516335 + 0.443489i$	$0.154318 - 0.489842i$	1.72876
$-0.991547$	$1.65225$	2.79015
$1.0874i$	$-2.12728$	3.06668
$-0.70143 + 0.965223i$	$-0.739773 - 2.58049i$	3.30279
$1.36576 + 0.578827i$	$3.36485 + 3.37562i$	3.86627
$1.76288i$	$-7.38429$	4.31192
$0.865622 + 1.64001i$	$-4.66799 + 6.98328i$	4.43945
$-1.94374$	$9.50289$	4.55665
$-1.69376 + 1.27953i$	$3.32987 - 11.3531i$	4.77895

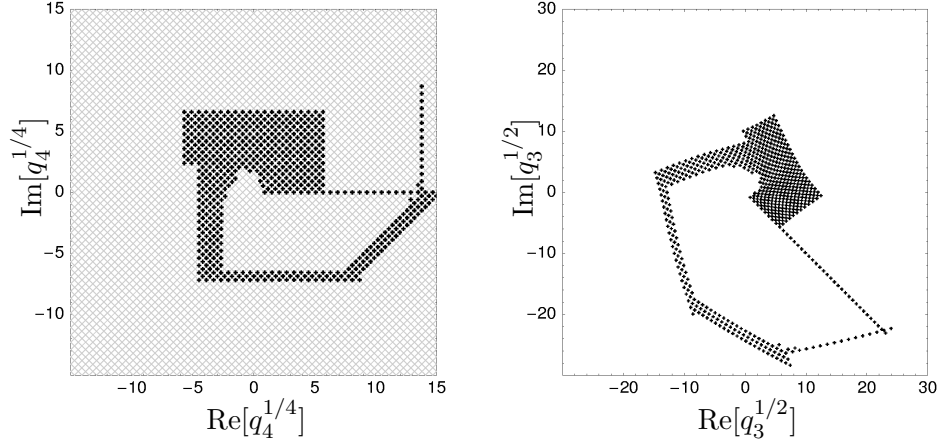
 Table 1. Resemblant lattice state spectrum for  $n_h = 1$  and  $\theta_4 = 0$ .


Figure 6. Parts of the winding spectra of the conformal charges for  $n_h = 1$  with  $\theta_4 = 0$ . On the left panel the spectrum of  $q_4^{1/4}$ , while on the right panel the spectrum of  $q_3^{1/2}$ . To show clearly winding correspondence we plot the WKB lattice with only some “random” vertices. However, the eigenvalues are related to all vertices except vertices in the vicinity of  $q_4 = q_3 = 0$ .

be degenerated [16], the ground state should have  $q_3 = 0$ . Therefore, the ground state should belong to the  $n_h$  even sector. Indeed, the ground states for  $N = 4$  Reggeons has conformal Lorentz spin  $n_h = 0$  [22].

## 6. Point-like solutions

It turns out that there are also other solutions for  $\nu_h = 0$  which do not lie on trajectories. These specific solutions will be called in the following point-

$q_3$	$q_4$	$E_4/4$
$-1.36248i$	$0.67053$	$1.59563$
$2.48686 + 0.45641i$	$-0.673897 + 1.09776i$	$2.35448$
$1.80352 + 1.62846i$	$-0.599893 - 0.511892i$	$2.71937$
$1.00697 + 2.71392i$	$1.24653 - 1.72595i$	$2.97916$
$-4.24348i$	$4.86137$	$-3.82033$
$4.75145 + 0.852837i$	$-3.64269 + 2.82969i$	$3.82631$
$3.81467 + 2.64475i$	$-3.76349 - 2.18733i$	$3.90119$
$5.70668 - 1.4752i$	$0.745664 + 6.40784i$	$4.10895$
$-2.79806 + 4.31936i$	$0.348195 + 6.24031i$	$4.15134$
$6.35987 - 4.68879i$	$8.48213 + 6.07874i$	$4.61273$

Table 2. Winding lattice state spectrum for  $n_h = 1$  and  $\theta_4 = 0$ .

like solutions. They appear for special values of conformal charges with  $n_h \neq 0$  for which in order to form four independent solutions less logarithmic terms are needed. All these solutions do not have any continuation in the  $\nu_h$ -real space.

### 6.1. Point-like solutions with even $n_h$ for $q_3 = 0$ and $\nu_h = 0$

For  $h = (1 + n_h)/2$  where  $n_h \in 2\mathbb{Z}$  there are two solutions with integer roots of the indicial equation (41), *i.e.*  $b_1 = 0$  and  $b_2 = 1$ , and two solutions with half-integer roots, *i.e.*  $b_3 = 4s - h - 1$  and  $b_4 = 4s + h - 2$ . In this situation according to (61) we have usually one  $\text{Log}(1-z)$  solution. However, there are special values of conformal charges for which recurrence relations produce the fourth independent non- $\text{Log}(1-z)$  solutions. In the case  $n_h = 2$  we have the following condition

$$64q_4 - 3 + 64q_3^2 = 0, \quad (62)$$

corresponding to the point-like solutions, and for  $n_h = 4$

$$36864q_4^2 + (5760 + 40960q_3^2)q_4 - 1215 + 1152q_3^2 + 4096q_3^4 = 0. \quad (63)$$

Going farther, the conditions have a form of polynomials of the order  $n_h/2$  in  $q_4$  and  $n_h$  in  $q_3$ .

Substituting  $q_3 = 0$  to the above conditions it turns out that in this case the quantization conditions (46) are satisfied. Resulting solutions for  $q_4$  as well as energies are given in Table 3. All these solutions have  $\theta_4 = 0$ . The energy minimum corresponds to the solution with

$$h = \frac{5}{2}, \quad q_3 = 0, \quad q_4 = -0.275767 \quad \text{with} \quad E_4/4 = -4.448118. \quad (64)$$

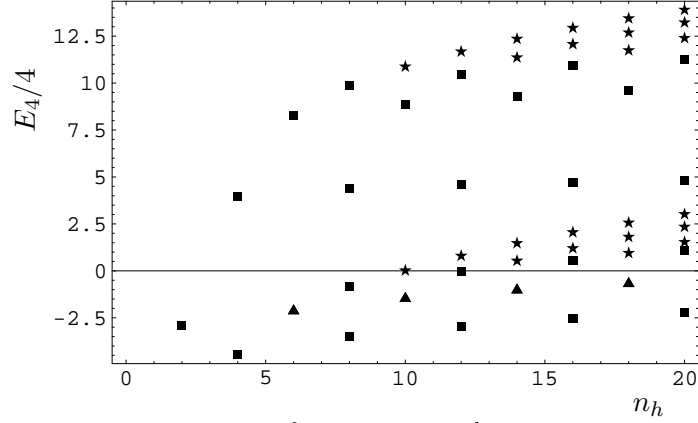


Figure 7. The energy spectrum for point-like solutions with  $n_h \in 2\mathbb{Z}$  and  $q_3 = 0$ . Here, shapes correspond to different degeneration of the spectrum.

$n_h$	$q_4$	$E_4/4$
<b>4</b>	<b>-0.275767</b>	<b>-4.48118</b>
	0.119517	3.95157
$n_h$	$q_4$	$E_4/4$
2	0.046875	-2.93147
6	0.845724	8.27268
	$0.147451 + 0.545843i$	-2.13355
	$0.147451 - 0.545843i$	-2.13355
10	1.811503	8.88331
	17.565015	0.0193639
	17.696871	10.87678
	$0.0804929 - 1.267133i$	-1.47238
	$0.0804929 + 1.267133i$	-1.47238
14	3.085760	9.28477
	26.493695	0.537166
	26.923075	11.36316
	90.973271	1.47330
	90.985515	12.35532
	$-0.066595 - 2.190390i$	-1.02327
	$-0.066595 + 2.190390i$	-1.02327
18	4.653448	9.58289
	36.621504	0.95062
	37.532130	11.74430
	124.243665	1.80846
	124.289745	12.68904
	283.831799	2.56459
	283.832674	13.44736
	$-0.291545 - 3.302932i$	-0.682788
	$-0.291545 + 3.302932i$	-0.682788
$n_h$	$q_4$	$E_4/4$
8	4.793879	-0.832250
	5.188999	9.87791
	-0.777194	-3.50838
	0.481816	4.37493
12	-1.477392	-2.93906
	1.092692	4.59523
	7.441803	-0.05004
	8.672696	10.47907
	43.879856	0.80083
16	43.921595	11.67925
	-2.359361	-2.53521
	1.973521	4.72661
	10.290397	0.56333
	12.827684	10.91734
	62.689999	1.20368
	62.835700	12.07543
20	167.556849	2.05481
	167.560211	12.93746
	-3.412519	-2.22192
	3.150012	4.80588
	13.265811	1.07723
	17.609886	11.26143
	83.859313	1.53510
	84.184263	12.39907
	220.781025	2.34429
	220.794663	13.22664
	451.493039	3.01760
	451.493257	13.90039

Table 3. The energy spectrum and  $q_4$  values for  $n_h \in 2\mathbb{Z}$  and  $q_3 = 0$ . The lowest energy solution is in bold.

Note that solution (64) has energy close to two Pomerons:  $2E_2/4 = -5.54518$  and it is lower than the Pomeron energy, *i.e.* with higher intercept. For given

$n_h \in 2\mathbb{Z}$  the number of such solutions is  $|n_h/2|$ . The energy spectrum is plotted in Fig. 7. One can see that increasing conformal Lorentz spin  $n_h$  the energy goes up.

### 6.2. Point-like solutions with even $n_h$ for $q_3 \neq 0$ and $\nu_h = 0$

Additionally to solutions with  $q_3 = 0$  we have also point-like solutions with  $q_3 \neq 0$ . Conformal charges of these solutions can be plotted as vertices of one WKB lattice. One can see their structure in Fig. 8. The solutions with  $n_h = 2$  satisfy conditions (62) and for large  $q_4$  and  $q_3$  WKB conditions (49) and (50) are satisfied. Condition (62) changes  $q_4^{1/4}$ -lattice to  $q_3^{1/2}$ -lattice rotated by  $\pm\pi/4$  up to a small shift vanishing for large  $q_k$ . Due to different roots in  $q_3^{1/2}$  and  $q_4^{1/4}$  as well as symmetry  $q_k \leftrightarrow q_k^*$  two points in the  $q_4^{1/4}$ -lattice correspond to one point in the  $q_3^{1/2}$ -lattice. On the other hand, points in the  $q_4^{1/4}$ -lattice are degenerated with respect to  $\theta_4 = \pi/2, 3\pi/2$ . Conformal charges for a few first solutions are presented in Table 4.

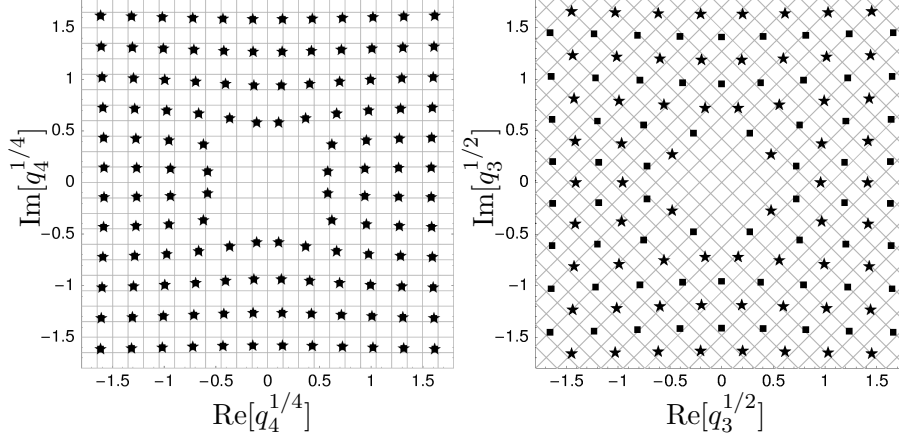


Figure 8. The spectra of the conformal charges for  $n_h = 2$  with  $\theta_4 = 3\pi/2$  (stars) and  $\theta_4 = \pi/2$  (boxes). On the left panel the spectrum of  $q_4^{1/4}$ , while on the right panel the spectrum of  $q_3^{1/2}$ .

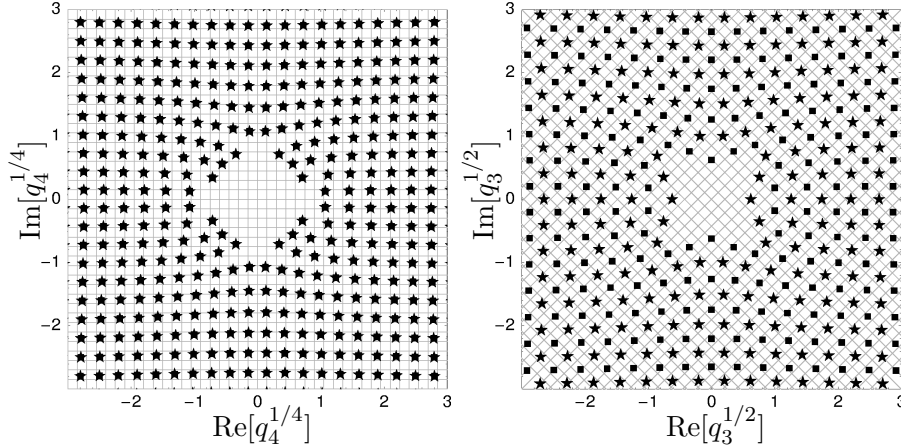
For  $n_h = 4$  we have point-like solutions whose conformal charges satisfy (63). Taking this condition for  $q_4 \rightarrow \infty$  and  $q_3^2/q_4 \sim 1$  we obtain

$$9q_4^2 + 10q_3^2q_4 + q_3^4 = 0 \quad (65)$$

which gives two solutions. The first solution,  $q_3^2 = -9q_4$ , is related to a lattice with  $|\ell_3| = 3$  while the second one,  $q_3^2 = -q_4$ , corresponds to a lattice



$q_3$	$q_4$	$E_4/4$
$0.154083 - 0.260344i$	$0.0909123 + 0.0802291i$	0.0420484
$-0.494888 + 0.230748i$	$-0.144794 + 0.228388i$	1.05762
$-0.256542 + 0.839351i$	$0.685571 + 0.430658$	2.07086
0.914503	-0.78944	2.10239
$0.791746 + 0.730241i$	$-0.0467357 - 1.15633i$	2.45655
$-1.37191 + 0.462032i$	$-1.62178 + 1.26773i$	3.04034
$0.357736 + 1.5676i$	$2.37626 - 1.12157i$	3.26625
$-1.0851 + 1.43035i$	$0.91534 + 3.10414i$	3.48118
1.98735	-3.90267	3.67686
$1.83956 + 1.13559i$	$-2.04755 - 4.17796i$	3.84871

 Table 4. Point-like solution spectrum for  $n_h = 2$ ,  $q_3 \neq 0$  and  $\theta_4 = 3\pi/2$ .

 Figure 9. The spectra of the conformal charges for  $n_h = 4$ ,  $|\ell_3| = 1$  with  $\theta_4 = 3\pi/2$  (stars) and  $\theta_4 = \pi/2$  (boxes). On the left panel the spectrum of  $q_4^{1/4}$ , while on the right panel the spectrum of  $q_3^{1/2}$ .

with  $|\ell_3| = 1$ . The lattice with  $|\ell_3| = 1$  is plotted in Fig. 9 and Table 5 and the lattice with  $|\ell_3| = 3$  in Fig. 10 and Table 6.

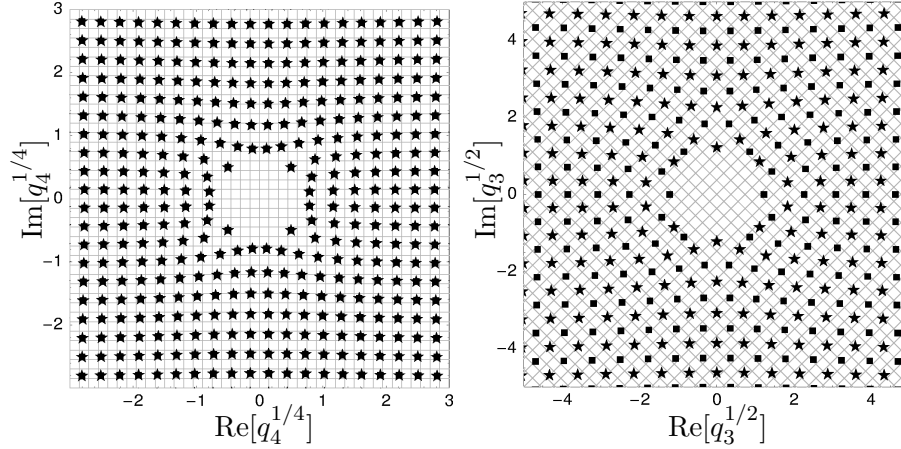
Moreover, additionally to these point-like solutions one can find descendent solutions, which have  $q_4 = 0$ , *e.g.* a point-like solution with  $h = 5/2$  where

$$q_3 = \pm i3\sqrt{5}/8, \quad \theta_4 = \pi, \quad E_4/4 = -1.158883, \quad (66)$$

or with  $h = 7/2$  where

$$q_3 = \pm 3\sqrt{35}/8, \quad \theta_4 = \pi, \quad E_4/4 = 5.50778. \quad (67)$$

$q_3$	$q_4$	$E_4/4$
0.386612	-0.388714	-0.393603
$0.450425 + 0.532463i$	$-0.0847377 - 0.377046i$	1.30653
$-0.961493 - 0.362284i$	$-0.961366 - 0.677412i$	2.13479
$0.264113 + 1.18142i$	$1.2114 - 0.611009i$	2.91603
$-0.83545 - 1.13937i$	$0.46445 - 1.88396i$	3.0377
1.5859	-2.67051	3.10799
$1.50126 + 0.951915i$	$-1.49397 - 2.84724i$	3.4103

Table 5. Point-like solution spectrum for  $n_h = 4$ ,  $|\ell_3| = 1$ ,  $q_3 \neq 0$  and  $\theta_4 = 3\pi/2$ .Figure 10. The spectra of the conformal charges for  $n_h = 4$ ,  $|\ell_3| = 3$  with  $\theta_4 = 3\pi/2$  (stars) and  $\theta_4 = \pi/2$  (boxes). On the left panel, where boxes coincide with stars, the spectrum of  $q_4^{1/4}$ , while on the right panel the spectrum of  $q_3^{1/2}$ .

$q_3$	$q_4$	$E_4/4$
$0.502865 + 1.89451i$	$0.345943 - 0.217117i$	1.05203
-1.49327	-0.246831	1.80272
$-1.68063 - 1.69926i$	$-0.0085373 - 0.641561i$	1.83642
$3.26053 - 1.1522i$	$-1.04678 + 0.836881i$	2.71529
$-0.890225 - 4.04854i$	$1.7154 - 0.801894i$	2.85804
$2.75764 + 3.74489i$	$0.697135 - 2.29665i$	3.15922
-5.12753	-2.93541	3.45247

Table 6. Point-like solution spectrum for  $n_h = 4$ ,  $|\ell_3| = 1$ ,  $q_3 \neq 0$  and  $\theta_4 = 3\pi/2$ .

The descendent point-like solutions for  $N = 4$  reggeized gluons come from the  $N = 3$  point-like solutions with the same quantum numbers and the same energy<sup>9</sup>.

### 6.3. Point-like solutions with odd $n_h$ for $\nu_h = 0$

For  $n_h = 1$  and  $q_3 = 0$  there is one lattice for point-like solutions with:

$$v_m(y) = y^{b_m} \sum_{n=0}^{\infty} v_n^{(m)} y^n,$$

$$v_{m+2}(y) = y^{b_{m+2}} \sum_{n=0}^{\infty} v_n^{(m+2)} y^n + \text{Log}(y) v_m(y), \quad (68)$$

where  $m = 1, 2$ , while  $b_1 = 1$ ,  $b_2 = 0$ ,  $b_3 = -1$ ,  $b_4 = -2$  for  $s = 0$  and  $b_1 = 3$ ,  $b_2 = 2$ ,  $b_3 = 1$ ,  $b_4 = 0$  for  $s = 1$ . The corresponding quantum values of  $q_4$  and  $E_4/4$  for point-like solutions are plotted in Fig. 11. One can see that the solution with the lowest energy  $E_4/4 = -1.03996$  corresponds to  $(\ell_1, \ell_2) = (2, 0)$ . Additionally, we have solutions with  $q_2 = q_3 = q_4 = 0$  and  $E_4 = 0$  as well as  $\theta_4 = \pi$  with the  $z = 1$  solutions  $Q_i^{(1)}(z) = z^{1-s}(1 - z)^{b_i} \sum_{n=0}^{\infty} v_n^{(i)}(1 - z)^n$ .

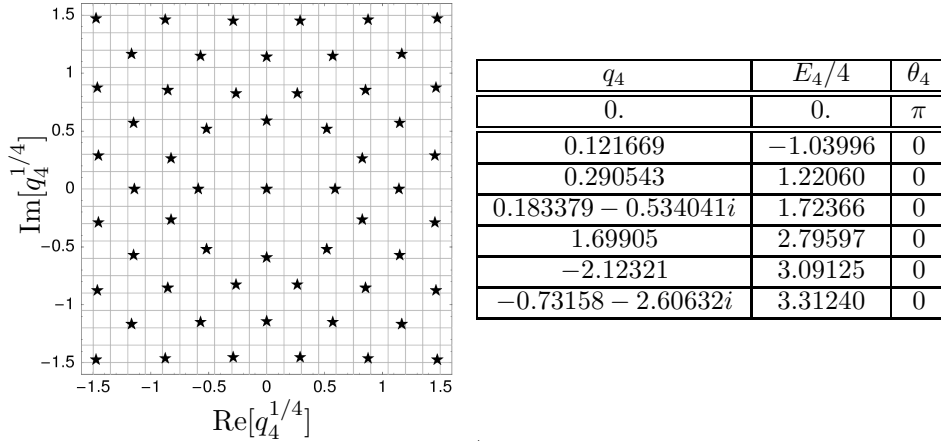


Figure 11. The spectrum of quantized  $q_4^{1/4}$  for the system with  $n_h = 1$  and  $q_3 = 0$ .

For odd  $|n_h| > 1$  we have also WKB lattices of point-like solutions. For example point-like solutions with  $q_3 = 0$  are plotted in Fig. 12. On the other hand, Fig. 13 and Table 7 show an example of point-like rotated lattices.

<sup>9</sup> If the  $N = 3$  point-like solutions with the quantum numbers (66) had been normalizable the odderon intercept of the three reggeized gluon would be higher than one.

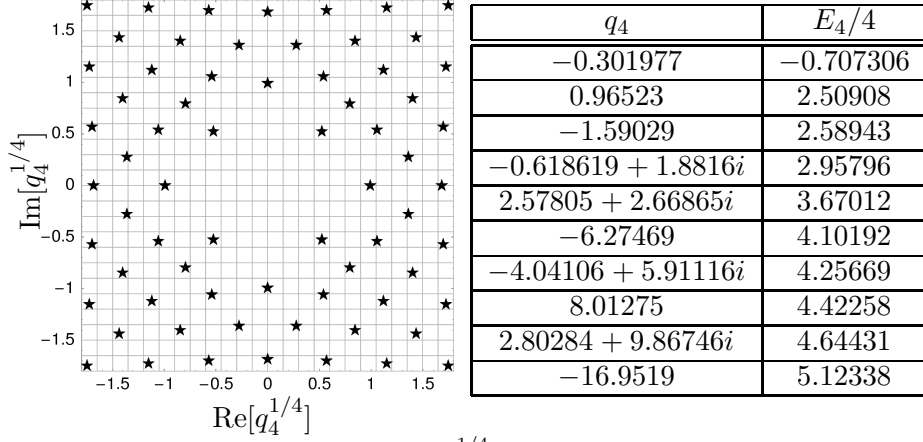


Figure 12. The spectrum of quantized  $q_4^{1/4}$  for point-like solutions with  $n_h = 3$  and  $q_3 = 0$ .

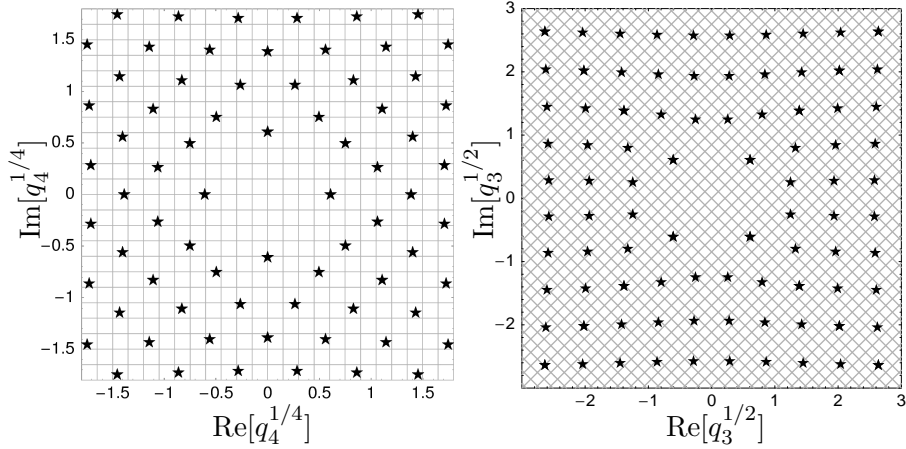
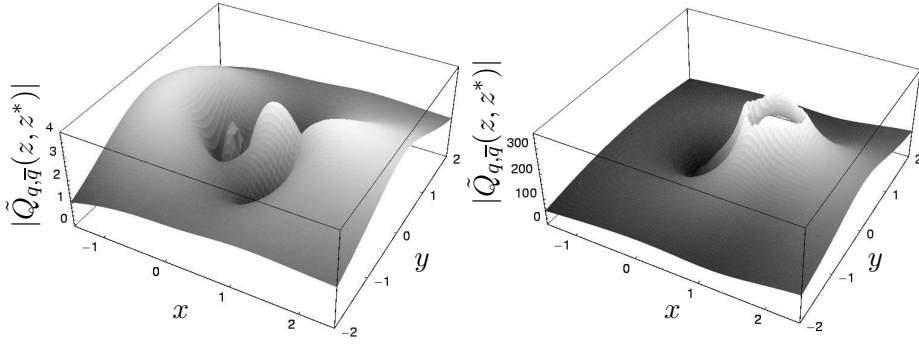


Figure 13. Point-like rotated spectra of the conformal charges for  $n_h = 3$  with  $\theta_4 = 0$ . On the left panel the spectrum of  $q_4^{1/4}$ , while on the right panel the spectrum of  $q_3^{1/2}$ .

## 7. Examples of norm calculation

The eigenfunctions  $\tilde{Q}_{q,\bar{q}}(z, z^*)$  presented in Section 5 whose conformal charges form trajectories are finite on the whole complex  $z$ -plane. One of such functions is shown on the left panel in Fig. 14. The norm of these trajectory solutions is infinite for  $\nu_h = \nu'_h$ . However, they describe continuous spectra so it is natural that they are normalized to the Dirac delta function (30).

$q_3$	$q_4$	$E_4/4$
$-0.73865i$	0.136401	0.634391
$1.48983 - 0.636904i$	$-0.453486 + 0.474439i$	1.96712
$1.12055 - 2.11477i$	$0.804151 + 1.18485i$	2.63622
$3.84094i$	3.68821	3.59751
$3.66894 - 1.07472i$	$-3.07653 + 1.97155i$	3.62067
$3.13679 - 3.30259i$	$0.266913 + 5.17977i$	3.95358
$1.94306 - 5.67594i$	$7.11021 + 5.51436i$	4.50006
$6.54514 - 1.4747i$	$-10.166 + 4.82605i$	4.73498
$5.94333 - 4.46239i$	$-3.85257 + 13.2607i$	4.93545
$8.1565i$	16.6321	5.11626

Table 7. Point-like solution spectrum for  $n_h = 3$  and  $\theta_4 = 0$ .Figure 14. The Baxter eigenfunctions  $\tilde{Q}_{q,\bar{q}}(z, z^*)$  with  $z = x + iy$ . The trajectory-like solution with  $h = 3/2$ ,  $q_3 = 0$  and  $q_4 = 1.4100348$  is plotted on the left panel, while on the right panel we plot the point-like solution with  $h = 3/2$ ,  $q_3 = 0$  and  $q_4 = 3/64$ .

On the other hand there exist solutions that do not form trajectories in real  $\nu_h$ . An example of the point-like eigenfunction  $\tilde{Q}_{q,\bar{q}}(z, z^*)$  with  $h = 3/2$ ,  $q_3 = 0$  and  $q_4 = 3/64$  is plotted on the right panel in Fig. 14. One can see a strong singularity at  $z = z^* = 1$ , which is present for all point-like solutions. These solutions appear only for  $\nu_h = 0$ , therefore, they have to be normalizable to the Kronecker delta symbol while their norm (48) has to be finite for all quantum numbers. It turns out that only series solutions around  $z = 1$  can give infinite contribution to the norm (48). Series around  $z = 0$  and  $z = \infty$  due to their asymptotics give at most finite contribution. Let us therefore consider calculation of contribution to norm from solutions around  $z = 1$ .

### 7.1. Point-like solutions with odd $n_h$

The solution for  $h = 1$  and  $q_3 = 0$  and  $q_4 \neq 0$  around  $z = 1$  has a form  $\tilde{Q}_{q,\bar{q}}(z, \bar{z}) = \overline{Q}_i(\bar{z}) C_{ij}^{(1)} Q_j(z)$ , with  $Q_i(z) = z^{(1-s)} v_i(1-z)$  and (68). From singlevaluedness condition we get that:

$$C^{(1)} = \begin{pmatrix} X_1 & X_2 & X_5 & X_7 \\ X_3 & X_4 & X_6 & X_8 \\ X_5 & X_7 & 0 & 0 \\ X_6 & X_8 & 0 & 0 \end{pmatrix}. \quad (69)$$

From numerical calculation one can see that  $X_6 = X_7 = 0$  and  $X_2 = X_3$ . The other ones may be different from zero. The most singular contribution comes from the term

$$\tilde{Q}_{q,\bar{q}}(z, \bar{z}) = X_8 z v_4(1-z) \bar{v}_2(1-\bar{z}) + \dots = X'_8 z(1-z)^{-2} (1-\bar{z})^2 + \dots, \quad (70)$$

where  $X'_8 = X_8 h_0^{(4)} \bar{h}_0^{(2)}$ . Substituting (70) to (48) one obtains

$$\begin{aligned} \langle q, \bar{q} | q, \bar{q} \rangle &= 48 D^6 \left( \prod_{i=1}^3 \int_{\rho}^R \rho_i d\rho_i \int_0^{2\pi} d\phi_i \right) \\ &\times \frac{\prod_{j < k} (\rho_j e^{i\phi_j} - \rho_k e^{i\phi_k})(\rho_j e^{-i\phi_j} - \rho_k e^{-i\phi_k})}{\rho_1^4 \rho_2^4 \rho_3^4} + \dots, \quad (71) \end{aligned}$$

with  $D \sim X'_8$  and where we perform the integrals around  $z_i = \bar{z}_i = 1$  from radius  $\rho \rightarrow 0$  up to radius  $R$  with  $z_j = 1 + \rho_j e^{i\phi_j}$  and  $\bar{z}_i = 1 + \rho_j e^{-i\phi_j}$ . Evaluating the integrals one gets

$$\langle q, \bar{q} | q, \bar{q} \rangle \sim \lim_{\rho \rightarrow 0} R^2 \frac{\log(\rho/R)}{\rho^2} + \dots \log(\rho/R) + \dots, \quad (72)$$

*i.e.* the singularity at  $\rho \rightarrow 0$ . The other terms give finite results around  $\rho = 0$  so the above singularity cannot be cancelled. Such solutions are non-normalizable. Similarly one can calculate the norm of the other point-like solutions with  $n_h \in 2\mathbb{Z} + 1$ .

### 7.2. Point-like solutions with even $n_h$

For point-like solutions with even  $n_h$  we can perform similar calculations but here we don't have logarithmic solutions. The solution around  $z = 1$  has a form:  $\tilde{Q}_{q,\bar{q}}(z, \bar{z}) = \overline{Q}_i(\bar{z}) C_{ij}^{(1)} Q_j(z)$ , with  $Q_i(z) = z^{(1-s)} v_i(1-z)$ , where

$$v_i(y) = y^{b_i} \sum_{n=0} h_n^{(i)} y^n, \quad (73)$$

with  $b_1 > b_2 > b_3 > b_4$ . The mixing matrix has a form

$$C^{(1)} = \begin{pmatrix} X_1 & X_2 & 0 & 0 \\ X_3 & X_4 & 0 & 0 \\ 0 & 0 & X_5 & X_6 \\ 0 & 0 & X_7 & X_8 \end{pmatrix}. \quad (74)$$

The divergent contribution comes from

$$\tilde{Q}_{q,\bar{q}}(z, \bar{z}) = X_8 z v_4 (1-z) \bar{v}_4 (1-\bar{z}) + \dots = X'_8 z (1-z)^{-5/2} (1-\bar{z})^{3/2} + \dots, \quad (75)$$

where in the second term of (75) the exponents are shown for the  $n_h = 2$  case.

Performing calculations similar to the case of odd  $n_h$  we obtain for  $n_h = 2$  logarithmic singularity

$$\langle q, \bar{q} | q, \bar{q} \rangle \sim \lim_{\rho \rightarrow 0} R^6 \frac{\log(\rho/R)}{\rho^6} + \dots \quad (76)$$

For point-like solutions with higher  $n_h \in 2\mathbb{Z}$  we obtain even stronger singularities, *i.e.*  $\langle q, \bar{q} | q, \bar{q} \rangle \sim \lim_{\rho \rightarrow 0} 1/\rho^{6n_h-6}$ .

To sum up, all point-like solutions constructed in Section 6 are non-normalizable because they do not have continuation in  $\nu_h \in \mathbb{R}$  and their norm is singular at  $\nu_h = 0$ . Thus, they do not belong to the Hamiltonian spectrum and therefore they do not contribute to the physical scattering processes.

### 7.3. Point-like solutions with infinite energy

Since in the analytical continuation of the energy there are poles for odd  $2i\nu_h$  one can expect that according to (56) this pole-solutions have twin-solutions for  $\nu_h \in \mathbb{R}$  and odd  $n_h$ . Indeed, such point-like solutions also appear.

Let us consider the first pole with  $q_3 = q_4 = 0$ ,  $n_h = 0$  and  $i\nu_h = 3/2$ , *i.e.*  $(h, \bar{h}) = (2, 2)$ . It should have a twin-solution with  $(h, \bar{h}) = (2, -1)$  and  $q_3 = q_4 = 0$ . Solving the differential equations (32) and resuming the series we obtain

$$\tilde{Q}_{q,\bar{q}}(z, \bar{z}) = \alpha_1 \frac{z(z+1)}{(1-z)^3} + \alpha_2 \left( \frac{z(z+1)}{(1-z)^3} \text{Log}[z\bar{z}] + \frac{2z}{(1-z)^2} \right) \quad (77)$$

where  $\alpha_3 = \alpha_4 = 0$  in Eq. (39) and  $\alpha_1, \alpha_2$  are arbitrary constants. Using Eq. (34) one can find that solution proportional to  $\alpha_1$  have  $\theta_4 = \pi$  while one at  $\alpha_2$  have  $\theta_4 = 0$ . Considering (40) one cannot evaluate their energy, *i.e.*  $E_4 = \pm\infty$ .

Similar solutions exist for other energy poles. Applying Eq. (48) to these pole-like solutions one gets the vanishing norm. Thus, these solutions also do not contribute to the physical processes.

### Summary

We have focused on four-Reggeon exchanges with the non-vanishing conformal Lorentz spin,  $n_h$ . These exchanges contribute to the elastic amplitude processes. In this work the energy spectrum of the exchanged states as well as the spectrum of conformal charges have been calculated, which enabled to calculate high energy behaviour of the scattering amplitude. The Reggeized gluon states contribute also to processes of deep inelastic scattering of a virtual photon  $\gamma^*(Q^2)$  off a hadron with mass  $M^2$  where  $\Lambda_{QCD} \ll M^2 \ll Q^2$ . With the help of techniques presented in this paper it is possible to calculate the anomalous dimensions of QCD for the structure function. This can be achieved by performing analytical continuation of the energy  $E_4(\nu_h)$  in to the complex  $\nu_h$ -plane and compute expansion coefficients of the energy around its poles [4, 5]. Positions of these poles describe possible values of the twist while the coefficients set a dependence of anomalous dimensions on the strong coupling constant. To this end, the first step is the same as in the case of Eq. (1), *i.e.* to solve the Schrödinger equation (6) using Baxter  $Q$ -operator method.

To find the energy spectrum (*i.e.* intercepts) and conformal charges, the Baxter eigenproblem was numerically solved. It turns out that apart from the ordinary states, which form one dimensional trajectories in the space of conformal charges along  $\nu_h$  direction, there exist other solutions to the Baxter equation, *i.e.* the point-like solutions. In order to contribute to the scattering amplitude processes, *i.e.* to be physical, the pertinent solutions should be normalizable according to the  $SL(2, \mathbb{C})$  scalar product. Thus, the scalar product of the trajectory solutions with continuous parameters  $\nu_h$  and  $\nu'_h$  has to be proportional to  $\delta(\nu_h - \nu'_h)\delta_{n_h n'_h}$  while the scalar product of the point-like solutions to the Kronecker delta  $\delta_{n_h n'_h}$ . On the other hand by construction, the wave-functions of the eigenstates should have transformation property w.r.t.  $SL(2, \mathbb{C})$  conformal transformations, *i.e.* they have to be homogeneous functions of two-dimensional coordinates and should not involve any scale. These conditions are not met by discrete spectrum. Since the discrete point-like solutions have infinite or vanishing norm, they are non-normalizable and they do not belong to the physical spectrum of the Hamiltonian. Moreover, they do not contribute to the physical processes.

The point-like states have been considered in Ref. [6, 15] as candidates for the ground-states which would give the main contribution to the scattering processes. There are no point-like solutions for the vanishing conformal Lorentz spin. However, such solutions appear for  $n_h \neq 0$ .

These discrete solutions appear due to the symmetry of Casimir operator namely  $\bar{h} \leftrightarrow 1 - \bar{h}$  which may throw solutions outside the physical region. This symmetry is valid only for (half-)integer conformal weights  $(h, \bar{h})$ . The



main issue is how a given solution to the conditions (57) looks like in the vicinity of  $h, \bar{h} \in \mathbb{Z}/2$ . If one solves the quantization conditions for  $h = (1-n_h)/2$  and  $\bar{h} = (1+n_h)/2$  then one should be prepared to encounter both physical, *i.e.* normalizable solutions as well as non-physical non-normalizable ones. The only way to distinguish them is to move a little bit away from these values of  $h$  and  $\bar{h}$  and check if they are situated on some physical trajectory with  $\nu_h \in \mathbb{R}$ .

The only physical spectrum of the Hamiltonian (2) is continuous spectrum. This spectrum may be parameterized using WKB approximation performed for large values of conformal charges. The energy states depend on continuous parameter  $\nu_h$ , integer conformal Lorentz spin  $n_h$  and a set of integer parameters which enumerate the trajectories as a vertices of WKB lattices. The energy of the states with  $n_h \neq 0$  is always higher than energy of ground state in the  $n_h = 0$  sector. However  $n_h \neq 0$  sectors may give the leading contribution to the scattering amplitude if the ground state does not couple to scattered particles.

We hope that this work explains the situation of four reggeized gluon solutions for  $n_h \neq 0$ . Although the point-like solutions do not contribute to the scattering amplitudes they are a very interesting part of the Baxter eigenproblem. We have to remember about them solving  $SL(2, \mathbb{C})$  system in the future. One can expect that the point-like solutions may also appear for  $N \neq 4$  Reggeon solutions. Finally, we have to agree with [11] that in the multi-colour limit the four-Reggeon state with the lowest energy which governs the four Reggeon physical scattering processes lies on the trajectory (64) from the  $n_h = 0$  sector with  $q_3 = 0$  and  $E_4 = -2.69664$ .

### Acknowledgements

I would like to warmly thank to G. P. Korchemsky, A. N. Manashov and M. Praszalowicz for fruitful discussions and help during preparation of this work. This work was supported by the grant of the Polish Ministry of Science and Education P03B 024 27 (2004-2007).

## Appendix A

### Recurrence relations for $u_n^{(k)}$

#### Appendix A.1 Coefficients $u_n^{(k)}$ around $z = 0$

The coefficient for the recurrence relations around  $z = 0$  are defined as follows

$$a_{0,n} = -2(n-s+1)^4 - \sum_{k=2}^4 i^k q_k (n-s+1)^{4-k}, \quad (\text{A.1})$$

$$a_{-1,n} = (n-2s+1)^4, \quad (\text{A.2})$$

$$a_{1,n} = (n+1)^4, \quad (\text{A.3})$$

while

$$a_{i,n}^{(k)} = \frac{d^k}{dn^k} a_{i,n}. \quad (\text{A.4})$$

Now, in Eq. (37)  $u_{-1}^{(k)} = 0$ ,  $u_0^{(k)} = 1$  and  $u_m^{(k)} \equiv u_m^{(k)}(q)$  is defined by

$$\begin{aligned} u_m^{(k)} a_{1,m-1} &= -u_{m-1}^{(k)} a_{0,m-1} - u_{m-2}^{(k)} a_{-1,m-1} \\ &\quad - \sum_{i=1}^{k-1} \frac{1}{(k-i)!} (u_m^{(i)} a_{1,m-1}^{(k-i)} + u_{m-1}^{(i)} a_{0,m-1}^{(k-i)} + u_{m-2}^{(i)} a_{-1,m-1}^{(k-i)}), \end{aligned} \quad (\text{A.5})$$

with

$$u_k(z) = (k-1)! z^{1-s} \sum_{n=0}^{\infty} u_n^{(k)} z^n. \quad (\text{A.6})$$

Finally, one obtains Eq. (36).

#### Appendix A.2 Coefficients $v_m^{(j)}$ around $z = 1$

The coefficient for the recurrence relations around  $z = 1$  can be defined as

$$A_{1,n} = (-1+n)n(2-h+n-4s)(1+h+n-4s), \quad (\text{A.7})$$

$$\begin{aligned} A_{2,n} &= -(n(6+3n(5+n(4+n)))+iq_3+h(1+2n-2s)-28s-8n(7+3n)s \\ &\quad +8(6+7n)s^2-32s^3+h^2(-1-2n+2s)), \end{aligned} \quad (\text{A.8})$$

$$\begin{aligned} A_{3,n} &= 14+n(39+n(40+3n(6+n)))+iq_3+q_4+h(1+n-s)^2-h^2(1+n-s)^2 \\ &\quad -60s-(4n(34+n(25+6n))+iq_3)s+32(1+n)(3+2n)s^2-4(17+16n)s^3+18s^4, \end{aligned} \quad (\text{A.9})$$

$$A_{4,n} = -(2 + n - 2s)^4, \quad (\text{A.10})$$

while

$$A_{i,n}^{(k)} = \frac{d^k}{dn^k} A_{i,n}. \quad (\text{A.11})$$

For non- $\text{Log}(1-z)$  solutions we have recurrence relations for  $v_m^{(i)} \equiv v_m^{(i)}(q)$  from Eq. (53):

$$\sum_{k=0}^3 v_{m-k}^{(i)} A_{k+1,m-k+b_i} = 0, \quad (\text{A.12})$$

where  $b_i$  are corresponding roots of indicial equation and  $A_{k,m}$  are defined above. The solutions with one- $\text{Log}(1-z)$  term have coefficients  $v_m^{(i)}$  defined as

$$\sum_{k=0}^3 v_{m-k}^{(i)} A_{k+1,m-k+b_i} + \sum_{k=0}^3 v_{m-k-d_{ij}}^{(j)} A_{k+1,m-k+b_i}^{(1)} = 0, \quad (\text{A.13})$$

where  $d_{ij} = b_i - b_j$  while the index  $j$  is related with the solutions at one- $\text{Log}(1-z)$  term (see Eq. 68). Finally, the coefficients of two- $\text{Log}(1-z)$  solutions, *i.e.*  $v_m^{(i)}$  have following constraints

$$\begin{aligned} \sum_{k=0}^3 v_{m-k}^{(i)} A_{k+1,m-k+b_i} + \sum_{k=0}^3 v_{m-k-d_{ij}}^{(j)} A_{k+1,m-k+b_i}^{(1)} \\ + \sum_{k=0}^3 v_{m-k-d_{il}}^{(l)} A_{k+1,m-k+b_i}^{(2)} = 0, \end{aligned} \quad (\text{A.14})$$

where  $b_l < b_j < b_i$  and the index  $j$  is related with the solutions at one- $\text{Log}(1-z)$  term while  $l$  corresponds to the solution at two- $\text{Log}(1-z)$  term. Moreover, one has to fix one coefficient for each solution, *i.e.* usually  $v_0^{(i)} = 1$ , and one coefficient for the each  $\text{Log}(1-z)$  term.

If  $A_{k,m}^i = 0$  for some  $i, k, m$  then recurrence relations may be closed. In this situation to calculate  $v_m^{(k)}$  one has to solve a set of linear equations. Moreover, these linear equation also can give additional constraints on conformal charges. This is mechanism of point-like solution appearing. Such solutions have usually less  $\text{Log}(1-z)$  terms than normal one.

## References

- [1] M. Gell-Mann, M.L. Goldberger, F.E. Low, E. Marx, F.Zachariasen. *Phys. Rev. B*, 133:145, 1964; M. Gell-Mann, M.L. Goldberger, F.E. Low, E. Marx, F.Zachariasen. *Phys. Rev. B*, 133:161, 1964.

- [2] V. N. Gribov. *Sov. Phys. JETP*, 26:414–422, 1968; J. Bartels. *Phys. Lett.*, B68:258, 1977; H. Cheng, C. Y. Lo. *Phys. Rev.*, D15:2959, 1977.
- [3] V. S. Fadin, E. A. Kuraev, L. N. Lipatov. *Phys. Lett.*, B60:50–52, 1975; E. A. Kuraev, L. N. Lipatov, V. S. Fadin. *Sov. Phys. JETP*, 44:443–450, 1976; E. A. Kuraev, L. N. Lipatov, V. S. Fadin. *Sov. Phys. JETP*, 45, 1977; I. I. Balitsky, L. N. Lipatov, *Sov. J. Nucl. Phys.*, 28:822–829, 1978.
- [4] T. Jaroszewicz. *Phys. Lett.*, B116:291, 1982.
- [5] G. P. Korchemsky, J. Kotanski, A. N. Manashov. *Phys. Lett.*, B583:121–133, 2004.
- [6] H. J. De Vega, L. N. Lipatov. *Phys. Rev.*, D66:074013, 2002. hep-ph/0204245v1.
- [7] J. Bartels. *Nucl. Phys.*, B175:365, 1980; J. Kwiecinski, M. Praszalowicz. *Phys. Lett.*, B94:413, 1980; T. Jaroszewicz. *Acta Phys. Polon.*, B11:965, 1980.
- [8] L. N. Lipatov. *JETP Lett.*, 59:596–599, 1994.
- [9] L. D. Faddeev, G. P. Korchemsky. *Phys. Lett.*, B342:311–322, 1995.
- [10] S. E. Derkachov, G. P. Korchemsky, A. N. Manashov. *Nucl. Phys.*, B617:375–440, 2001.
- [11] S. E. Derkachov, G. P. Korchemsky, J. Kotanski, A. N. Manashov. *Nucl. Phys.*, B645:237–297, 2002.
- [12] S. E. Derkachov, G. P. Korchemsky, A. N. Manashov. *Nucl. Phys.*, B661:533–576, 2003.
- [13] Jan Kotanski. *Acta Phys. Polon.*, B37:2655–2693, 2006.
- [14] Jan Kotanski. 2005. The PhD Thesis, hep-th/0511279.
- [15] H. J. De Vega, L. N. Lipatov. hep-ph/0204245v2.
- [16] G. P. Korchemsky. *Nucl. Phys.*, B443:255–304, 1995.
- [17] G. 't Hooft. *Nucl. Phys.*, B72:461, 1974; L. N. Lipatov. *Phys. Lett.*, B251:284–287, 1990; L. N. Lipatov. *Phys. Lett.*, B309:394–396, 1993.
- [18] L. N. Lipatov. *JETP Lett.*, 59:596–599, 1994.
- [19] R. J. Baxter. *Exactly Solved Models in Statistical Mechanics*. Academic Press, London, 1982.
- [20] E. K. Sklyanin. 1991. hep-th/9211111.
- [21] J. Kotanski, M. Praszalowicz. *Acta Phys. Polon.*, B33:657–682, 2002.
- [22] G. P. Korchemsky, J. Kotanski, A. N. Manashov. *Phys. Rev. Lett.*, 88:122002, 2002.